C.P. No. 140
(15,400)
A.R.C. Technical Report

MINISTRY OF SUPPLY

AERONAUTICAL RESEARCH COUNCIL

CURRENT PAPERS

The Measurement of Heat Transfer and Skin Friction at Supersonic Speeds

Part IV. Tests on a Flat Plate at M = 2.82

By

R. J. Monaghan and J. R. Cooke

LONDON: HER MAJESTY'S STATIONERY OFFICE

1953

Price 8s. 0d. net

C.P. No. 140

CORRIGENDA

Section 5.2 Temperature Distributions

In the above section use is made of temperature-velocity distributions suggested by Squire[8]. These distributions incorporate the index "n" of the power-law velocity distribution, which is normally of the order of 1/7. It must be stressed therefore that the curve labelled "n = 0" in Fig.14 has no physical significance and should only be regarded as giving an absolute lower (or upper) bound to the theoretical values.

Setting n = 0 in formulae such as for recovery factor is only justified on the grounds of its being a convenient and (in most cases) sufficiently accurate approximation.

28th September, 1953

C.P. No. 140

Technical Note No. Aero 2171

June, 1952

ROYAL AIRCRAFT ESTABLISHMENT

The measurement of heat transfer and skin friction at supersonic speeds

Part IV - Tests on a flat plate at M = 2.82

by

R. J. Monaghan
and
J. R. Cooke

SUMMARY

This note gives the results of overall heat transfer and boundary layer measurements made on a flat plate in a 5 in. square supersonic wind tunnel operating at M = 2.82 under atmospheric stagnation pressure conditions. The tests were made to extend the range of results previously obtained at M = 2.43[1,2] and used the same experimental equipment.

In general the results confirm those obtained at the lower Mach number and some general conclusions are now drawn concerning the structure and behaviour of experimental laminar and turbulent compressible boundary layers on a flat plate.

The present series of tests is now complete, but subsonic check tests remain to be made.

LIST OF CONTENTS

APPENDIX

LIST OF TABLES

LIST OF ILLUSTRATIONS

1 Introduction

This note gives the results of overall heat transfer and boundary layer measurements made on a flat plate in a 5 in. square supersonic wind tunnel operating at M = 2.82 with atmospheric stagnation pressure. The tests were made to extend the range of the results previously obtained at M = 2.43[1,2] and used the same experimental equipment.

The overall heat transfer measurements were made with a mean plate temperature of approximately 373°K and for tunnel stagnation temperatures in the range 225°K to 312°K, corresponding to free stream Reynolds numbers between 2.5 and 4 million, based on plate length.

Pressure and temperature traverses of the boundary layer were made for the zero heat transfer condition and for one case with heat transfer (T_w = 373°K, T_{H_1} = 276.5°K). These have been analysed to show the characteristics of the boundary layer and an additional analysis is made of the velocity and temperature distributions. The latter are also compared with results obtained by Spivack[3] from measurement of a tunnel wall boundary layer at M = 2.8.

The tests were made between August and December 1950 and in February 1951 and complete the present series, but subsonic check tests are to be made and there may be an extension to higher Mach numbers and Reynolds numbers at a future date.

2 Experimental apparatus and techniques

The tunnel (apart from the higher Mach number nozzle), hot plate and heating equipment, and pressure and temperature measuring equipment were the same as described in Ref.2.

This section is concerned with the flow over the plate given by the new nozzle and with a slight refinement in the method of deriving total temperatures from the recorded pitot-thermocouple temperatures in the boundary layer.

2.1 Mach number distribution along plate

The Mach number distribution along the plate, as derived from surface static and tunnel stagnation pressures, was as shown in Fig.1. The variation from the average mean Mach number of 2.82 was less than ±2 per cent in all cases, but this is larger than would normally be considered acceptable by present standards for a general purpose tunnel.

However the approximate calculations of Appendix I suggest that the resulting errors (due to pressure gradients) in the turbulent boundary layer should always be less than 2 per cent, provided Reynolds numbers etc are based on local conditions. Such an error is within the limits of experimental accuracy and the Mach number variation was therefore accepted for the present series of check tests.

The errors in the laminar boundary layer over the forward portion of the plate are not so easy to assess, but since they are complicated by additional effects discussed below, and since the experimental accuracy is lower than in the turbulent layer further back, the effects of possible pressure gradients have been neglected.

The plate was raised 0.16 inches above wall level as in the M_1 = 2.43 tests[1,2], at which height at least 96 per cent (by velocity) of the tunnel wall boundary layer was removed by suction at its leading

edge. Thus some residual turbulence is left in the stream over the plate. Fig. 1 shows that the resulting Mach number distribution over the forward portion of the plate was better than that obtained in the same region of an unbroken flat wall. The slight dip in the region of 6 inches back from the leading edge is probably caused by disturbances arising at the points where the leading edge enters the side-wall boundary layers. (A similar effect was observed in the $M_1 = 2.43$ tests[2]). The more pronounced drop and subsequent recovery at 10 inches back occurs both on the plate and on the unbroken flat wall and is presumably caused by a small irregularity in the nozzle profile. It is possible that this disturbance may come from the plug in one of the forward holes cut in the liner to accommodate the pitot holder. As made, the plugs were a flush fit, but in time a small amount of distortion always occurs between a wooden plug and wooden liner. However its effect on the boundary layer should theoretically be less than 2 per cent, as has already been mentioned.

2.2 Pitot-thermocouple recovery factors

The design of the combined pitot and thermocouple tube was the same as described in Ref. 2, but a standard sized head of about 0.017 in. outside diameter was used throughout the present tests. The required small air-flow through the tube during temperature readings was obtained as in Ref. 2 by opening the connection to a vacuum pump. The flow quantity should then depend on the difference

$$p_o' - p_{vac}$$

between pitot pressure (p_o') and pump pressure p_{vac}. During a boundary layer traverse, p_{vac} remained sensibly constant but p_o' varied between 50 and 250 mm.Hg.abs. To allow for this, the pitot-thermocouple was calibrated in the free stream over the full range of pressure differences ($p_o' - p_{vac}$) producing curves, such as shown in Fig. 2, for recovery factor β_{th}. (For definitions of the symbols used in this note, see the list of symbols at the back). A separate calibration was made for each traverse since small differences were found, but the general shape was close to that illustrated. This shows that β_{th} varied between 0.92 and 0.94 over the range of ($p_o' - p_{vac}$) of the traverses, and the calibration was then assumed to apply through the boundary layer.

An alternative procedure would be to keep ($p_o' - p_{vac}$) constant during the traverse, but this would mean accepting the lower value of $\beta_{th} = 0.92$ throughout.

The highest value of $\beta_{th} = 0.94$ was less than that obtained for a pitot-thermocouple of similar dimensions in the $M_1 = 2.43$ tests. This may be a Mach number effect, or it may be caused by slight differences in the geometry of the quartz pitot heads and positioning inside them of the thermo-junction. The latter explanation is supported indirectly by Spivack's results[3], which show no systematic variation in the recovery factor of his temperature probe between M = 1.2 and M = 2.8.

3 Overall heat transfer tests

3.1 Measurement of kinetic temperature rise

The method used in Ref. 2 for determining kinetic temperature rise was to circulate room air through the plate and to vary the tunnel stagnation temperature slowly until the inlet and outlet temperatures of the circulating air coincided, when zero heat transfer conditions were assumed to have been reached. The method was not very satisfactory and in the present tests an attempt was made to measure the kinetic temperature rise directly from the surface temperatures of the copper plate. Since the plate is mounted in a wall of the tunnel, zero heat transfer conditions between plate and air-stream will only be obtained if there is zero heat transfer between plate and room. Therefore the tunnel stagnation temperature was adjusted to make the mean plate surface and room temperatures equal, giving the results shown in Fig. 3a. As in the $M_1 = 2.43$ tests, there was a fall in surface temperature from leading edge to trailing edge.

Tests were also made using a dummy wooden plate, which is more nearly an insulated surface, giving results also shown in Fig. 3a. Surface temperatures measured on the wooden plate are considered to be less accurate than those measured on the copper plate, because it is difficult to instal the thermo-junctions so that they will read the actual surface temperature and not a mean temperature over a finite depth. This is not so serious with copper which is an excellent conductor, but wood is an insulator so that there can be large temperature gradients through it which can introduce sizeable errors. Hence the discrepancies shown between the two cannot be regarded as significant: the main conclusion is that the two sets of temperatures are of the same order of magnitude for the same stagnation temperature.

Local recovery factors (β) based on the copper plate surface and tunnel stagnation temperatures of Fig. 3a and the appropriate Mach number distribution of Fig. 1a, are given in Fig. 3b. The mean value is approximately 0.90, as compared with 0.906 (obtained by the circulation method) for $M_1 = 2.43$.

Finally, Fig. 3c shows the variation in mean recovery factor obtained when the stagnation temperature was varied, giving mean plate temperatures unequal to room temperature. Assuming that the heat transfer between plate and airstream varies as $(T_w - T_{wo})$ and the heat transfer between plate and room varies as $(T_w - T_R)$, (where T_w is the mean plate temperature, T_{wo} its zero heat transfer value and T_R is room temperature), then when equilibrium is established it can be shown that

$$\beta' = \bar{\beta} + A\,(T_R - T_w)$$

where β' is the apparent mean recovery factor based on T_w

and $\bar{\beta}$ is the true mean recovery factor for $T_w = T_{wo}$.

The scatter of the experimental points* in Fig. 3c shows the difficulty in obtaining an accurate estimate of $\bar{\beta}$, even though the

---

* The shape of the temperature distributions along the plate was similar to that of Fig. 3a in all cases.

temperatures were given at least half an hour to settle in each case. As a result, $\bar{\beta}$ is only specified to two places of decimals by

$$\bar{\beta} = 0.90 \tag{1}$$

and this value has been used in the analysis of the overall heat transfer results below.

3.2 Overall heat transfer results

Measurements of overall heat transfer were obtained as in Ref. 2 for a plate temperature of approx. 373°K and for tunnel stagnation temperatures in the range 225°K to 312°K. The results were analysed as in Ref. 2 (except that the mean recovery factor was taken to be 0.90) and are given in Table I, while Fig. 4 gives the plot of $k_h \, Re^{\frac{1}{5}}$ against $\frac{T_{H_1}}{T_w}$. (An auxiliary scale of $\frac{T_1}{T_w}$ is also given).

Colburn's formula

$$k_h = 0.036 \, \sigma^{-\frac{2}{3}} \, Re^{-\frac{1}{5}} \tag{2}$$

modified in accordance with the results of Ref. 1 to give (with $\sigma = 0.72$)

$$k_{hw} = 0.045 \left(Re_w \frac{T_1}{T_w} \right)^{-\frac{1}{5}} \tag{3}$$

gives good agreement with the experimental values in Fig. 4. However the trend of the latter indicates that for $\frac{T_{H_1}}{T_w}$ less than 0.60, ($\frac{T_1}{T_w}$ less than 0.43) equation 3 might underestimate the heat transfer. These conclusions are in agreement with those[2] obtained from the $M_1 = 2.43$ tests.

Note however that equation 2 is equivalent to taking

$$k_h = \left(\frac{1}{2} C_F \right) \sigma^{-\frac{2}{3}} \tag{4}$$

with C_F given by the Blasius' formula, whereas the Karman relation between skin friction and heat transfer would give

$$k_h = \left(\frac{1}{2} C_F \right) \sigma^{-\frac{1}{3}} \tag{5}$$

which for $\sigma = 0.72$ would give a line 10 per cent below that shown in Fig. 4. This emphasises the need for further heat transfer measurements from a flat plate at low speeds in order to establish the constant in equation 3.

4 Boundary layer measurements

Pressure and temperature traverses of the boundary layers corresponding to zero heat transfer conditions and to the heat transfer case $\frac{T_w}{T_{H_1}} = 1.35$ were obtained and analysed as in Ref. 2. The average pitot-thermocouple size was 0.017 in. O.D. but a number of pressure traverses were taken independently with a flattened stainless steel pitot head of height 0.010 in.

The present section considers transition position, and the variations of displacement and momentum thicknesses, etc. Section 5 below considers the structure of the velocity and temperature distributions across the turbulent boundary layer.

4.1 Transition position and velocity profiles

The results of creeper measurements of transition on the centre line of the plate are shown in Fig. 5.

Under zero heat transfer conditions $\left(\frac{T_w}{T_{H_1}} = 0.94\right)$ the transition region begins 4 in. from the leading edge at

$$Re_x = 0.8 \times 10^6.$$

For heat flow from the plate to the airstream $\left(\frac{T_w}{T_{H_1}} = 1.35\right)$, the transition region has moved forward and now begins at

$$Re_x = 0.45 \times 10^6$$

i.e. increase in $\frac{T_w}{T_{wo}}$ from 1 to 1.44 has almost halved the transition Reynolds number. This gives further emphasis to the importance of knowing the heat transfer conditions when making estimates of boundary layers occurring in supersonic flight. It also emphasises the need for further measurements of the movement of transition with heat transfer, but the present rig is unsuitable for such work because of the very low transition Reynolds number under zero heat transfer conditions.

Velocity profiles for the two experimental conditions are given in Figs. 6 and 7. As in the $M_1 = 2.43$ tests[1,2], the laminar profiles are "fuller" than theory[4] would predict. For zero heat transfer the turbulent profiles (Fig. 6) once again agree well with the $\frac{1}{7}$th power law, with the appropriate value of $\frac{\delta^x}{\delta}$ from Ref. 5. For $\frac{T_w}{T_{H_1}} = 1.35$, the $M_1 = 2.43$ results[2] agreed with a $\frac{1}{6}$th power law, but Fig. 7 does not show this trend except very close to the wall. Instead, the profiles at the beginning of the turbulent region are closer to a $\frac{1}{8}$th power law and tend to the $\frac{1}{7}$th power law as the distance along the plate is increased. A more complete discussion of the turbulent profiles, based on the log-law form, is given in section 5.

4.2 Displacement and momentum thicknesses, etc.

The variations along the plate of displacement and momentum thicknesses and of the shape parameter $H = \frac{\delta^x}{\theta}$ are given in Table II and in Figs. 8-10. The creeper measurements of section 4.1 determined transition position on the centre line, where the pitot traverses are normally made, but a test with an indicator showed that the transition region was tongue shaped as in Ref. 1, starting from the corners at the leading edge. Consequently a set of traverses was made along a line one inch off centre in the zero heat transfer case (Fig. 8) to test the validity of the assumption of two dimensional flow.

Fig. 8 shows close agreement between the two sets of traverses in the laminar region, but there is a divergence in the turbulent region. Such a divergence would be expected because of earlier transition on the line one inch off centre, and the curves show that the differences near the trailing edge of the plate could be consistent with this explanation. The difference in slopes between 4 and 8 inches from the leading edge cannot be explained as simply, unless there is a very long transition on the line one inch off centre. Also the possibility of secondary flows affecting the growth of turbulent boundary layer cannot be neglected. However the agreement in shape parameter H (Fig. 10) between the two sets of traverses, and the experimental agreement so far found with test results from other tunnels, both suggest that while the corner disturbances and possible secondary flows may affect transition position, the subsequent turbulent boundary layer is two dimensional in behaviour.

4.21 Laminar region

For zero heat transfer, the creeper gave the beginning of the transition region to be about 4 inches from the leading edge (Fig. 5), and ahead of this point there is fair agreement between theoretical[4] and experimental values of displacement thickness (δ^x, Fig.8). This is in contrast to the $M_1 = 2.43$ results[1] where the experimental values were about 25 per cent above the theoretical.

However the present and the earlier[1] results agree in showing experimental values of momentum thickness (θ) approximately 30 per cent above the theoretical (Fig. 8). Fig. 10 then shows that nowhere do the experimental values of H attain the theoretical[4] zero heat transfer laminar value of 8.1, appropriate to $M_1 = 2.82$.

Because of temperature measuring difficulties no traverses were obtained in the laminar region under heat transfer conditions (Fig. 9), but theoretically there should be little change in the values of θ as compared with the zero heat transfer case, although the values of H (and therefore of δ^x) should increase as shown in Fig. 10.

In the absence of pressure gradients, the mean skin friction coefficient (C_F) is obtained from momentum thickness (θ) by the formula

$$C_F = \frac{2\theta}{x} \qquad (6)$$

and Fig. 11 summarises the available data for its variation in a laminar boundary layer on a flat plate in a supersonic air-stream. The N.A.C.A. results are from interferometer and pitot measurements by Blue[6] on a flat

plate spanning the 3.6 inch square working section of a supersonic wind tunnel operating at M = 2.02 under zero heat transfer conditions. The pitot traverses were made with a tube 0.0026 in. high.

There is good agreement between the R.A.E. and N.A.C.A. results in showing skin friction coefficients 25 to 30 per cent above theoretical estimates. A possible explanation is that experimentally there is always a finite thickness and therefore a finite disturbance at the leading edge of a plate and the effect of this disturbance may be noticeable as a momentum loss in the boundary layer for some distance downstream. If it is assumed that this effect can be allowed for by the assumption that the effective start of the laminar boundary layer is upstream a distance x_o from the leading edge, then Fig. 11 shows that the experimental points are well fitted by taking $Re_{x_o} = 0.167 \times 10^6$. (This corresponds to $\frac{2}{3}$ inches in the R.A.E. tests at M = 2.43). Obviously a single value of Re_{x_o} could hardly suffice for all leading edge conditions or speeds, so to some extent the very close agreement between the R.A.E. results at M = 2.43 and Blue's results at M = 2.02 must be regarded as coincidental. However there is obviously definite support for the assumption that the effective start is upstream of the leading edge. The rising values of skin friction for $Re > 0.5 \times 10^6$, can be explained by the onset of transition.

4.22 Turbulent Region

The characteristics of the turbulent boundary layer (Figs. 8-10) confirm the results[1,2] of the $M_1 = 2.43$ tests, namely:

(1) in the zero heat transfer case (Fig. 8) values of momentum thickness derived from equation 6 above and the Ref. 1 formula

$$C_{F_w} = 0.46 \left(\log_{10} Re_w \frac{T_1}{T_w} \right)^{-2.6} \qquad (7)$$

agree well with experiment provided 0 is taken to be continuous with the experimental laminar value at a transition point given by the beginning of the transition region obtained from the creeper results of Fig. 5. (Equation 7 agrees with an earlier formula suggested by Cope for zero heat transfer conditions).

(2) no decrease in momentum thickness (and hence in skin friction) is found with heat transfer from plate to stream (Fig. 9), except indirectly through changes in free stream Reynolds number and in transition position.

(3) the shape parameter H (Fig. 10) is given reasonable accurately in both cases by the modified[2] Ref. 1 formula

$$H = 1.3 \left(\frac{T_w}{T_1} + \sigma^{\frac{1}{3}} \frac{\gamma - 1}{2} M_1^2 \right) \qquad (8)$$

and (4) values of displacement thickness can then be obtained by combining conclusions 1-3. (Figs. 8 and 9).

5 Analysis of velocity and temperature distributions in the turbulent boundary layer

The two major assumptions made in Ref. 1 when deriving formulae for the variations of skin friction etc with Mach number and heat transfer (equations 7 and 8 above) were

(1) that the general log law form for the turbulent velocity profile near a wall in incompressible flow

$$\frac{u}{u_\tau} = A + B \log_{10} y_\tau \qquad (9)$$

where

$$u = \left(\frac{\tau_o}{\rho}\right)^{\frac{1}{2}}$$

and

$$y_\tau = \frac{y u_\tau}{\nu} \quad ,$$

could be retained, with the same constants, in compressible flow provided density and viscosity were evaluated at wall temperature (giving u_{τ_w} and y_{τ_w}).

and (2) that Reynolds analogy between momentum and heat exchange was valid, giving the relations

$$T_H = T_{H_1} \qquad (10)$$

in the zero heat transfer case, and

$$\frac{T_w - T_H}{T_w - T_{H_1}} = \frac{u}{u_1} \qquad (11)$$

when heat is being transferred.

The results of Ref. 2 showed that neither assumption was valid, other than as a rough approximation. The present results check with this conclusion and are presented below.

5.1 Velocity distributions

Using values of $C_f \left(= 2 \frac{d\theta}{dx} \right)$ derived from Figs. 8 and 9, experimental values of $\frac{u}{u_{\tau_w}}$ and y_{τ_w} have been calculated from the measured velocity distributions. These values are tabulated in Table III and are plotted

in Fig. 12. As shown by the solid lines, good agreement is obtained by using equation 9 with values of A and B given by the following table, (also included in the table are the experimental values[2] obtained for $M_1 = 2.43$)

Temperature conditions	$M_1 = 2.43$		$M_1 = 2.82$	
	A	B	A	B
Zero heat transfer	5.45	5.4	5.9	5.0
$\frac{T_w}{T_{H_1}} = 1.35$	3.65	5.6	4.8	5.2
$\frac{T_w}{T_{H_1}} = 1.57$	1.65	6.1	-	-

These compare with the usual incompressible values of

$$A = 5.8 \text{ or } 5.5$$

and

$$B = 5.5 \text{ or } 5.75$$

The broken lines in Fig. 12 correspond to the values of A and B obtained in the $M_1 = 2.43$ tests[2] for the appropriate temperature conditions, and these also are seen to be in fair agreement with the present experimental values. Thus the above table should only be regarded as giving the order of the values of the constants A and B. It shows therefore that the assumption of Ref. 1 in retaining the incompressible constants is reasonably valid under zero heat transfer conditions up to $M_1 = 2.82$, but goes astray when heat is being transferred.

A number of authors have made theoretical investigations of the compressible turbulent boundary layer and a good summary of their assumptions and results is given by Rubesin, Maydew and Varga in Ref. 7*. Their report shows that the results obtained vary considerably with the initial assumptions made concerning both the equation for shearing stress and the boundary conditions at the junction with the laminar sub-layer or with the buffer layer. Thus by making suitable assumptions it might be possible to fit the experimental velocity profiles obtained in the present note and in Ref. 2, but such an investigation is beyond the scope of the present note since it raises fundamental questions concerning the mechanism of turbulence in a compressible flow.

5.2 Temperature Distributions

5.21 Zero heat transfer ($T_w = T_{wo}$)

Typical distributions of total temperature (T_H) as measured across the turbulent boundary layer under zero heat transfer conditions

---

* This report also contains experimental results for skin friction on a flat plate in a 6 in. tunnel at M = 2.5 and zero heat transfer conditions. These results are fitted well by the formula of Ref. 1, i.e. equation 7 of the present note.

are shown plotted against distance from surface in Fig. 13a and against velocity squared in Fig. 14. Both show the degree of departure from the simple assumption of constant total energy,

$$T_H = T_{H_1} \tag{10}$$

as normally used in analysis of boundary layer traverses.

Now in Ref. 2 it was shown that Squire's suggested temperature distribution[8] for the turbulent boundary layer under zero heat transfer conditions is equivalent to

$$T_H' = T + \sigma^{\frac{3n-1}{n+3}} \frac{u^2}{2Jg\ C_p} \tag{12}$$

$$= \text{constant}$$

$$= T_{wo} \text{ if correct values near the wall are desired,}$$

where

$$T_{wo} = T_1 + \sigma^{\frac{n+1}{n+3}} \frac{u_1^2}{2Jg\ C_p} \tag{13}$$

and "n" is the index in the power law velocity profile

$$\frac{u}{u_1} = \left(\frac{y}{\delta}\right)^n .$$

(Note that $T_H' = T_{wo}$ under zero heat transfer conditions, but when heat is being transferred, section 5.22 below, T_H' as defined by equation 12 will vary across the layer whereas T_{wo} will remain constant, being given by equation 13).

Following equations 12 and 13, values of $\frac{T_H}{T_{H_1}}$ can be obtained as functions of $\frac{u}{u_1}$ and these are plotted in Fig. 14 for $n = \frac{1}{7}$ and for the limiting value $n = 0$. The result shows that the experimental temperatures lie nearest to the line corresponding to $n = 0$, i.e. to

$$T_H' = T + \sigma^{\frac{1}{3}} \frac{u^2}{2Jg\ C_p} \tag{12a}$$

Using an appropriate experimental velocity distribution $\frac{T_H}{T_{H_1}}$ as obtained from equation 12a is plotted against y in Fig. 13a, which gives a comparison in terms of the physical dimensions of the boundary layer. The reversal in the experimental temperature distributions near the surface of the copper plate remains unexplained. Subsequent check tests showed that it was not an accidental effect confined to a particular test series.

A drawback to the temperature distribution given by n = 0 (equation 12a) is that the energy distribution obtained from it does not integrate to give zero heat transfer. Neither does the experimental temperature distribution, as is evident from Fig. 13a. This point was discussed in Ref. 2, where it was shown that use of the distribution for $n = \frac{1}{7}$ (Fig. 14),

$$T_H' = T + \sigma^{\frac{1}{3}} \frac{u^2}{2Jg\, C_p} \qquad (12b)$$

with an arbitrary extrapolation for values of T_H greater than T_{H_1} (since T_H must equal T_{H_1} in the free stream) could give a true zero heat transfer energy distribution.

Thus the distribution corresponding to $n = \frac{1}{7}$ would seem preferable and Fig. 14 shows that while it is not in agreement with the present results, it gives very good agreement (up to $\frac{T_H}{T_{H_1}} = 1$) with results obtained by Spivack[3] from measurement of a tunnel wall boundary layer at M = 2.8. The exact heat transfer conditions were in doubt during Spivack's tests but he assumed that they were very close to zero heat transfer.

Thus in summary it can be said that the most accurate zero heat transfer temperature distribution is probably given by Squires distribution[8] (equation 12) with $n = \frac{1}{7}$ (equation 12b). However in application to experimental boundary layer analysis, current variations in values accepted for Prandtl number (σ) for air make the additional refinement of equation 12b over equation 12a (for n = 0) hardly justifiable and in most cases it is probably sufficiently accurate to accept the assumption of constant total energy (equation 10).

5.22 With heat transfer. $T_w = 373^oK$. $T_{H_1} = 276.5^oK$

In this case, Reynolds analogy between momentum and heat exchange gives

$$\frac{T_w - T_H}{T_w - T_{H_1}} = \frac{u}{u_1} \qquad (14)$$

In Ref. 2 it was shown that a better distribution is probably given by

$$\frac{T_w - T_H'}{T_w - T_{H_1}'} = \frac{u}{u_1} \quad f(\sigma) \tag{15}$$

where T_H' is given by equation 12a

$$T_H' = T + \sigma^{\frac{1}{3}} \frac{u^2}{2Jg\, C_p} \tag{12a}$$

and the trend of the experimental results[2] suggested that

$$f(\sigma) = \sigma^{-\frac{1}{3}} \tag{16}$$

might be a good approximation for $f(\sigma)$.

Fig. 15 shows the present experimental results plotted as $\frac{T_H}{T_{H_1}}$ against $\frac{u}{u_1}$ and compares them with

(1) Reynolds analogy, equation 14

(2) Equation 15 with $f(\sigma) = 1$

and (3) Equation 15 with $f(\sigma) = \sigma^{-\frac{1}{3}}$ (with $\sigma = 0.72$).

Of the three, equation 15 with $f(\sigma) = 1$, i.e.

$$\frac{T_w - T_H'}{T_w - T_{H_1}'} = \frac{u}{u_1} \tag{15a}$$

gives probably the best approximation to the experimental results in Fig. 15. Thus despite the results of Ref. 2 there is not yet sufficient evidence to justify choosing

$$f(\sigma) = \sigma^{-\frac{1}{3}} \tag{16}$$

in preference to

$$f(\sigma) = 1$$

and as will be evident from Fig. 15, Reynolds analogy (equation 14) should be sufficiently accurate for analysis of experimental measurements at least within the range of heat transfer conditions so far covered.

6 General Conclusions from the Present Test Series

On the basis of the experimental results obtained in Ref.1, 2 and the present note, the following general conclusions can be drawn concerning the compressible laminar and turbulent boundary layers found on a flat plate in the absence of pressure gradients. The test Mach numbers were 2.43 and 2.82.

LAMINAR BOUNDARY LAYER

(1) The experimental velocity profiles were "fuller" than theory would predict. (e.g. see Fig. 6).

(2) The present tests and some American tests[6] at M = 2.02 both gave laminar skin friction coefficients 25-30 per cent above theory (Fig. 11), which is probably caused by the disturbance originating from finite thickness of the leading edge of the plate.

TRANSITION

(3) There was a forward movement of transition with heat transfer from plate to stream, but very little backwards movement occurred[2] for heat transfer in the opposite direction. However the present rig is unsuitable for quantitative evaluation of this effect and further work is necessary.

(4) In the analysis of the turbulent boundary layer it was found best to make momentum thickness (θ) continuous with its experimental laminar value (from conclusion 2 above) at a "transition point" given by the beginning of the normal transition region (e.g. c.f. Figs. 5 and 8).

TURBULENT BOUNDARY LAYER

(5) Under zero heat transfer conditions the velocity profiles followed the $\frac{1}{7}$ th power law form. At $M_1 = 2.43$ and with heat transfer from plate to stream, the profiles varied through a $\frac{1}{6}$ th to a $\frac{1}{5}$ th power law form, but the same behaviour was not discernible at $M_1 = 2.82$.

The results were also plotted in log law form

$$\frac{u}{u_{\tau_w}} = A + B \log_{10} \frac{y u_{\tau_w}}{\nu_w}$$

and a variation in the constants A and B was found. (Tabulated in the present note).

(6) Under zero heat transfer conditions the Ref. 1 formula for the variation of mean skin friction coefficient

$$C_{F_i} = C_{F_w}$$

when

$$Re_i = Re_w \frac{T_1}{T_w}$$

(where "i" denotes incompressible values

"w" denotes that density and viscosity are evaluated at wall temperature T_w

and T_1 is free stream static temperature)

gave good agreement with experiment, when allowance was made (following conclusion 4) for the laminar boundary layer over the forward portion of the plate. It also gives agreement with the majority of results from other sources.

(7) Contrary to the prediction of the Ref. 1 formula quoted in conclusion 6, no decrease in skin friction was found when heat was being transferred from plate to stream.

(8) With or without heat transfer, the shape parameter $\left(H = \frac{\delta^*}{\theta}\right)$ was given reasonably accurately (e.g. Fig. 10) by the formula

$$H = 1.3 \left(\frac{T_w}{T_1} + \sigma^{\frac{1}{3}} \frac{\gamma-1}{2} M_1^2\right)$$

where σ is Prandtl number (= 0.72 for air).

(9) The mean temperature recovery factor $(\bar{\beta})$ for the plate, defined by

$$\bar{\beta} = \frac{T_{wo} - T_1}{T_{H_1} - T_1}$$

where T_{wo} is the mean plate temperature for zero heat transfer

and T_1, T_{H_1} are the free stream static and total temperatures respectively,

had the value 0.906 at $M_1 = 2.43$ and 0.90 at $M_1 = 2.82$. Contrary to expectation, the local values at the front of the plate (laminar region) were slightly higher than those at the back (turbulent region). (e.g. Fig. 3b). The figure recommended for application for turbulent boundary layers is 0.90.

(10) Overall heat transfer coefficients k_h based on the temperature difference $(T_w - T_{wo})$ showed a slight variation with temperature ratio $\frac{T_1}{T_w}$.

The formula

$$k_{h_w} = 0.045 \left(Re_w \frac{T_1}{T_w} \right)^{-\frac{1}{5}}$$

gave good agreement with experiment. (This formula is a generalisation of Colburn's incompressible flow formula in accordance with the variation suggested in Ref. 1 and conclusion 6 above for skin friction in compressible flow. However the constant requires checking by further subsonic tests).

(11) The temperature distribution across the zero heat transfer turbulent boundary layer was given approximately by

$$T_H' = T + \sigma^{\frac{1}{3}} \frac{u^2}{2Jg\ C_p} = \text{constant} = T_{wo}$$

Further evidence[3] suggests that the true distribution may be given more nearly by

$$T_H' = T + \sigma^{\frac{5}{11}} \frac{u^2}{2Jg\ C_p} = \text{constant} = T_{wo}$$

These distributions are as suggested by Squire[8] and correspond to taking exponents 0 and $\frac{1}{7}$ in the power law velocity profile.

(12) When heat is being transferred the temperature distribution is given roughly by

$$\frac{T_w - T_H'}{T_w - T_{H_1}'} = \frac{u}{u_1}$$

where T_H' is defined as in conclusion 11.

LIST OF SYMBOLS

x	distance along plate from leading edge
y	distance normal to plate
u	velocity parallel to plate at a point in the boundary layer
u_1	value of "u" in free stream outside boundary layer
u_τ	friction velocity $\left\{= \left(\frac{\tau_o}{\rho}\right)^{\frac{1}{2}}\right\}$
τ_o	local skin friction
F	total skin friction on length x
ρ	density (mass units)
μ	dynamic viscosity
C_F	mean skin friction coefficient, C_f local skin friction coefficient
Re	Reynolds number based on plate length and free stream values of ρ and μ
Re_x	ditto, based on length x
T	static temperature
T_H	total temperature $= T + \frac{u^2}{2Jg\ C_p}$
T_H'	$= T + \sigma^{\frac{3n+1}{n+3}} \frac{u^2}{2Jg\ C_p}$ when "n" is exponent in turbulent velocity profile $\frac{u}{u_1} = \left(\frac{y}{\delta}\right)^n$

SUBSCRIPTS

1	denotes free stream value
w	denotes plate surface (wall) value
wo	denotes wall value for zero heat transfer
Q	overall heat transfer rate
S	heated area of plate

$k_h = \frac{\frac{Q}{S}}{\rho_1 u_1 g\ C_p (T_w - T_{wo})}$ (convective heat transfer coefficient).

where g is acceleration due to gravity

and C_p is specific heat of air at constant pressure

σ Prandtl number $\frac{C_p \mu}{k}$, where k is thermal conductivity.

β temperature recovery factor for flat plate

$$= \frac{T_{wo} - T_1}{T_{H_1} - T_1}$$

β_{th} pitot-thermocouple recovery factor

$$= \frac{T_{th} - T}{T_H - T}$$

where T_{th} is measured temperature of thermocouple.

δ^x displacement thickness of boundary layer

$$= \int_0^\delta \left(1 - \frac{\rho u}{\rho_1 u_1}\right) dy$$

θ momentum thickness of boundary layer

$$= \int_0^\delta \frac{\rho u}{\rho_1 u_1} \left(1 - \frac{u}{u_1}\right) dy$$

H shape parameter $= \frac{\delta^x}{\theta}$

REFERENCES

No.	Author	Title, etc.
1	R.J. Monaghan and J.E. Johnson	The measurement of heat transfer and skin friction at supersonic speeds. Part II. Boundary layer measurements on a flat plate at M = 2.5 and zero heat transfer. A.R.C. Current Paper No. 64. Dec. 1949.
2	R.J. Monaghan and J.R. Cooke	The measurement of heat transfer and skin friction at supersonic speeds. Part III. Measurements of overall heat transfer and of the associated boundary layers on a flat plate at M_1 = 2.43. C.P. No.139. Dec. 1951
3	H.H. Spivack	Experiments in the turbulent boundary layer of a supersonic flow. TIB/P31952 N.A.A. Aerophysics Lab. Report CM-615 Los Angeles, Calif. Jan. 1950
4	R.J. Monaghan	An approximate solution of the compressible laminar boundary layer on a flat plate. R & M 2760. Nov. 1949
5	W.F. Cope and G.G. Watson	Preliminary measurements of the boundary layer in the 11" supersonic wind tunnel. R & M 2304. Aug. 1946
6	R.E. Blue	Interferometer corrections and measurements of laminar boundary layers in supersonic stream. N.A.C.A. Tech. Note 2110 Washington June, 1950
7	M.W. Rubesin R.C. Maydew and S.A. Varga	An analytical and experimental investigation of the turbulent boundary layer on a flat plate at supersonic speeds. N.A.C.A. Tech. Note 2305 Washington Feb. 1951
8	H.B. Squire	Heat transfer calculation for aerofoils. R & M No.1986 Nov. 1942

APPENDIX I

Approximate estimate of effects of experimental pressure gradient on turbulent boundary layer results

The momentum integral equation for two-dimensional compressible flow reads

$$\frac{\tau_o}{\rho_1 u_1^2} = \frac{d\theta}{dx} + \theta(H + 2)\,\frac{1}{u_1}\frac{du_1}{dx} + \frac{\theta}{\rho_1}\frac{d\rho_1}{dx}$$

or, since

$$c^2 = \frac{dp}{d\rho}$$

$$\rho_1 u_1 \frac{du_1}{dx} = -\frac{dp}{dx}$$

and

$$C_f = \frac{\tau_o}{\frac{1}{2}\rho_1 u_1^2}$$

we have

$$C_f = 2\frac{d\theta}{dx} - \theta(H + 2 - M_1^2)\,\frac{p_o}{q}\,\frac{d\left(\frac{p}{p_o}\right)}{dx} \qquad \text{I.1}$$

where $q = \frac{1}{2}\rho_1 u_1^2$.

Thus Mach number is seen to have considerable effect on the effect of pressure gradients. Under zero heat transfer conditions at M = 2.82 Fig. 10 shows

$$H \simeq 5.$$

Now Fig. 1 shows that between $x = 1$ and $x = 9$, M_1 decreases from 2.85 to 2.77 and therefore $\frac{p}{p_o}$ increases from 0.0341 to 0.0386. As an approximation assume that the variation in $\frac{p}{p_o}$ is linear, then

$$\frac{d\left(\frac{p}{p_o}\right)}{dx} = 5.625 \times 10^{-4}$$

and, substituting in equation 1,

$$C_f = 2\frac{d\theta}{dx} - 5.625 \times 10^{-4}\,(7 - M_1^2)\,\frac{p_o}{q}\,\theta$$

$$= 2\frac{d\theta}{dx} - A\theta \,. \qquad \text{I.2}$$

Taking experimental values of M_1 from Fig. 1 and of θ and $\frac{d\theta}{dx}$ from Fig. 8 we then have the following approximate values

x =	5	9
M_1 =	2.83	2.77
$-A$ =	1.45×10^{-5}	1.67×10^{-5}
θ =	5×10^{-3}	9×10^{-3}
$2\frac{d\theta}{dx}$ =	2.6×10^{-3}	2.4×10^{-3}
$-\frac{A\theta}{2\frac{d\theta}{dx}}$ =	0.55×10^{-2}	0.7×10^{-2}

This shows that under the present conditions, the error in C_f introduced by neglecting the pressure gradient and taking the simple formula

$$C_f = 2\frac{d\theta}{dx} \qquad \text{I.3}$$

will be less than one per cent which is well within the experimental accuracy. Note however that C_f is based on the <u>local</u> and not on the mean values of ρ_1 and u_1.

Similarly it can be shown that the mean skin friction coefficient (C_F) is given by

$$C_F = \frac{2\theta}{x} \qquad \text{I.4}$$

to a similar order of accuracy, provided ρ_1 and u_1 are given their values at the point x. This suggests that the same considerations should apply when evaluating local Reynolds numbers, as has been done in Table II.

In the range $x = 9$ to $x = 12$, Fig. 1 shows that

$$\frac{d\left(\frac{p}{p_0}\right)}{dx} \simeq -1.7 \times 10^{-3}$$

so that in this case the errors involved in using equations 3 and 4 should be less than two per cent which is acceptable.

The errors in the heat transfer case (Figs. 1 and 9) will be of the same order.

It should be noted that the smallness of the pressure gradient effect as estimated above is fortuitous in that the Mach number is in the right region to minimise the term

$$(H + 2 - M_1^2)$$

in equation I.1.

TABLE I

Results of overall heat transfer measurements

$M_1 = 2.82$

Reynolds number based on plate length = 13.4 in. = 0.340 metres
Heated area = 57.6 sq.in. = 3.72×10^{-2} sq. metres
Results are in chronological order with divisions between tests

T_{H_1} °K	T_w °K	T_{w_o} °K	Q kcal/sec	Re $\times 10^{-6}$	k_h $\times 10^3$
273.0	372.6	256.3	0.0914	3.12	1.92
273.1	372.5	256.4	0.0939	3.12	1.32
242.1	372.4	227.4	0.1190	3.64	1.28
242.5	372.5	227.7	0.1216	3.64	1.30
233.9	372.2	219.6	0.1217	3.80	1.22
238.1	372.6	223.6	0.1190	3.75	1.23
238.0	372.5	223.5	0.1179	3.75	1.23
247.5	372.2	232.4	0.1084	3.55	1.22
248.2	372.3	233.0	0.1090	3.55	1.22
253.2	371.8	237.7	0.1089	3.44	1.29
253.0	372.4	237.6	0.1067	3.44	1.25
258.1	372.5	242.4	0.1004	3.35	1.24
258.1	372.5	242.4	0.1004	3.35	1.24
282.7	372.8	265.5	0.0852	2.93	1.34
282.8	372.8	265.6	0.0860	2.93	1.35
294.4	372.8	276.5	0.0786	2.74	1.41
264.1	372.9	248.0	0.1009	3.21	1.32
264.2	372.9	248.1	0.0994	3.21	1.30
267.9	372.4	251.6	0.0975	3.14	1.33
268.0	372.6	251.7	0.0972	3.14	1.33
287.6	372.5	270.1	0.0810	2.84	1.35
288.2	372.6	270.7	0.0812	2.84	1.36
298.0	372.5	279.8	0.0750	2.70	1.41
298.1	372.5	279.9	0.0745	2.70	1.40
310.3	372.5	291.4	0.0654	2.54	1.43
312.0	372.5	293.0	0.0633	2.54	1.41
246.9	372.7	231.8	0.1124	3.54	1.26
247.4	372.7	232.3	0.1139	3.54	1.28
225.4	372.6	211.7	0.1284	3.99	1.21
225.5	372.6	211.7	0.1274	3.99	1.20

TABLE II

Results of boundary layer measurements

$M_1 = 2.82$

(a) Centre line. Zero heat transfer. $\left(\frac{T_w}{T_{H_1}} = 0.94,\ T_w \simeq 289^\circ K\right)$

x in.	$Re_x \times 10^{-6}$	δ^x in.	θ in.	H
1.25	0.25	0.0169	0.00223	7.58
2.95	0.59	0.0219	0.00314	6.97
4.55	0.88	0.0292	0.00458	6.38
6.45	1.37	0.0330	0.00703	4.69
8.50	1.76	0.0445	0.00858	5.19
10.05	1.96	0.0533	0.01118	4.77
11.30	2.26	0.0637	0.01330	4.79
13.40	2.56	0.0754	0.01460	5.16

(b) 1" off centre line. Zero heat transfer

x in.	$Re_x \times 10^{-6}$	δ^x in.	θ in.	H
1.20	0.24	0.0148	0.00210	7.05
2.90	0.58	0.0200	0.00312	6.41
4.60	0.94	0.0253	0.00478	5.29
6.35	1.34	0.0370	0.00778	4.76
8.20	1.66	0.0515	0.01083	4.76
11.20	2.16	0.0716	0.01420	5.04
13.40	2.59	0.0825	0.01660	4.97

(c) Centre line. With heat transfer. $T_w = 373^\circ K$. $T_{H_1} = 276.5^\circ K$

x in.	$Re_x \times 10^{-6}$	δ^x in.	θ in.	H
2.95	0.69	0.0254	0.00328	7.74
4.65	1.07	0.0345	0.00541	6.38
6.37	1.49	0.0512	0.00831	6.16
8.40	2.00	0.0630	0.01035	6.09
11.25	2.57	0.0844	0.01360	6.21
13.35	3.04	0.0921	0.01489	6.19

TABLE III

Log-law velocity distributions in turbulent boundary layer

$M_1 = 2.82$

(a) Zero heat transfer conditions. $T_{r} \triangleq 289^{\circ}K$, $T_{H_1} \triangleq 307^{\circ}K$

Mean Re = 0.2×10^6 per inch

$\varphi = u/u_{\tau_w}$ $\eta = yu_{\tau_w}/\nu w$

x = 8.5 in.	
φ	$\log_{10}\eta$
9.28	1.032
10.71	1.179
11.99	1.288
12.79	1.375
13.67	1.510
14.25	1.635
14.67	1.731
15.77	1.878
16.24	1.987
16.56	2.149
17.77	2.355
18.23	2.447
18.46	2.524
18.54	2.589
18.55	2.645

x = 10.05 in.	
φ	$\log_{10}\eta$
12.61	1.303
13.02	1.382
13.53	1.449
13.79	1.507
14.26	1.004
14.65	1.701
14.98	1.780
15.45	1.905
15.85	2.002
16.57	2.148
17.17	2.237
17.67	2.345
18.08	2.417
18.38	2.479
18.49	2.507
18.64	2.559
18.73	2.625
18.76	2.718

x = 13.4 in.	
φ	$\log_{10}\eta$
8.73	0.981
9.43	1.127
10.71	1.236
11.68	1.324
12.36	1.396
12.79	1.458
13.49	1.583
13.93	1.680
14.60	1.826
15.09	1.935
15.93	2.095
17.19	2.303
18.07	2.444
18.42	2.500
18.72	2.549
18.96	2.594
19.16	2.644
19.27	2.729

(b) With heat transfer. $T_w = 373^{\circ}K$. $T_{H_1} = 276.5^{\circ}K$.

Mean Re = 0.23×10^6 per inch

x = 8.4 in.	
φ	$\log_{10}\eta$
7.49	0.995
9.07	1.104
10.06	1.192
11.37	1.326
12.15	1.451
12.67	1.548
13.05	1.627
13.34	1.694
13.89	1.803
14.33	1.891
14.72	1.963
15.40	2.080
15.93	2.171
16.36	2.247
16.70	2.312
16.92	2.368
17.04	2.417
17.10	2.502

x = 11.25 in.	
φ	$\log_{10}\eta$
7.15	0.820
7.96	0.966
9.13	1.075
10.18	1.162
11.39	1.297
12.13	1.422
12.62	1.519
13.00	1.598
13.31	1.665
13.74	1.774
14.47	1.933
15.59	2.142
16.45	2.282
17.07	2.375
17.44	2.473
17.55	2.605
17.56	2.824

x = 13.55 in.	
φ	$\log_{10}\eta$
8.36	0.811
9.39	0.957
10.35	1.067
10.92	1.154
11.77	1.288
12.32	1.413
12.71	1.510
13.28	1.656
13.74	1.766
14.50	1.925
15.11	2.042
16.07	2.209
16.82	2.330
17.36	2.424
17.72	2.501
17.84	2.567
17.85	2.624

Wt.2078. CP140. K5. - Printed in Great Britain.

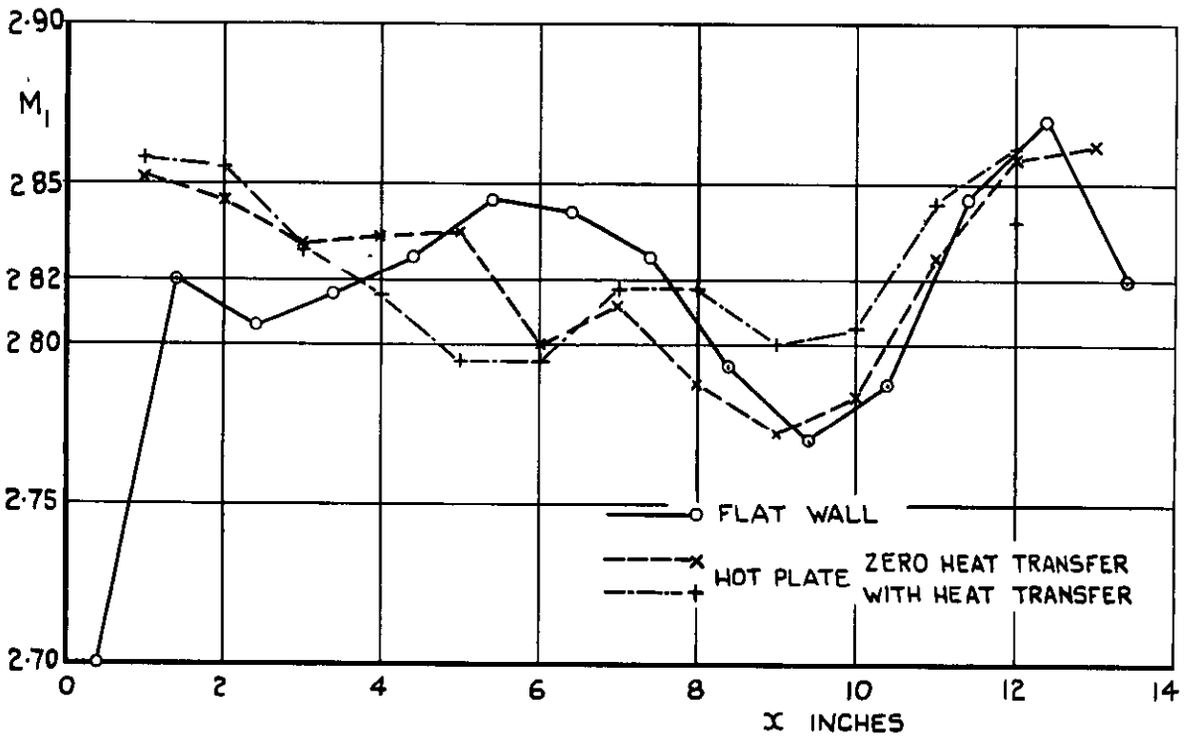

(a) MACH NUMBER DISTRIBUTION

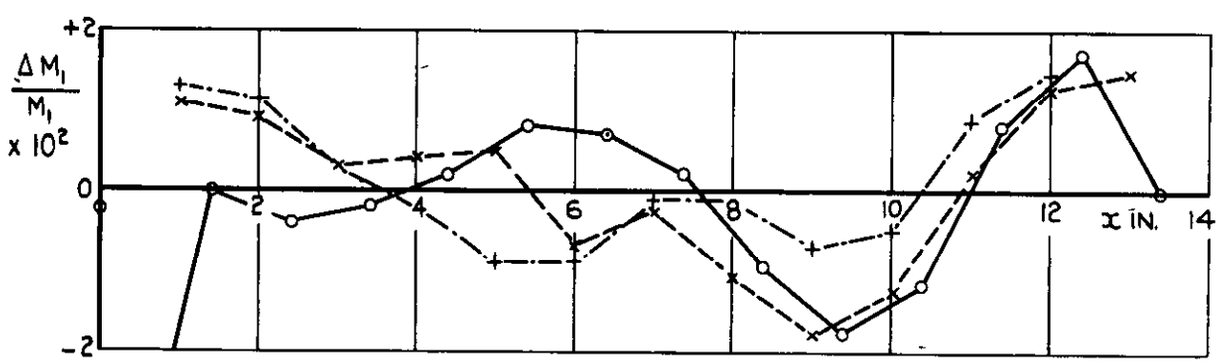

(b) PERCENTAGE VARIATION FROM MEAN $M_1 = 2{\cdot}82$

FIG. I(a & b) MACH NUMBER DISTRIBUTION ALONG PLATE.

FIG.2.

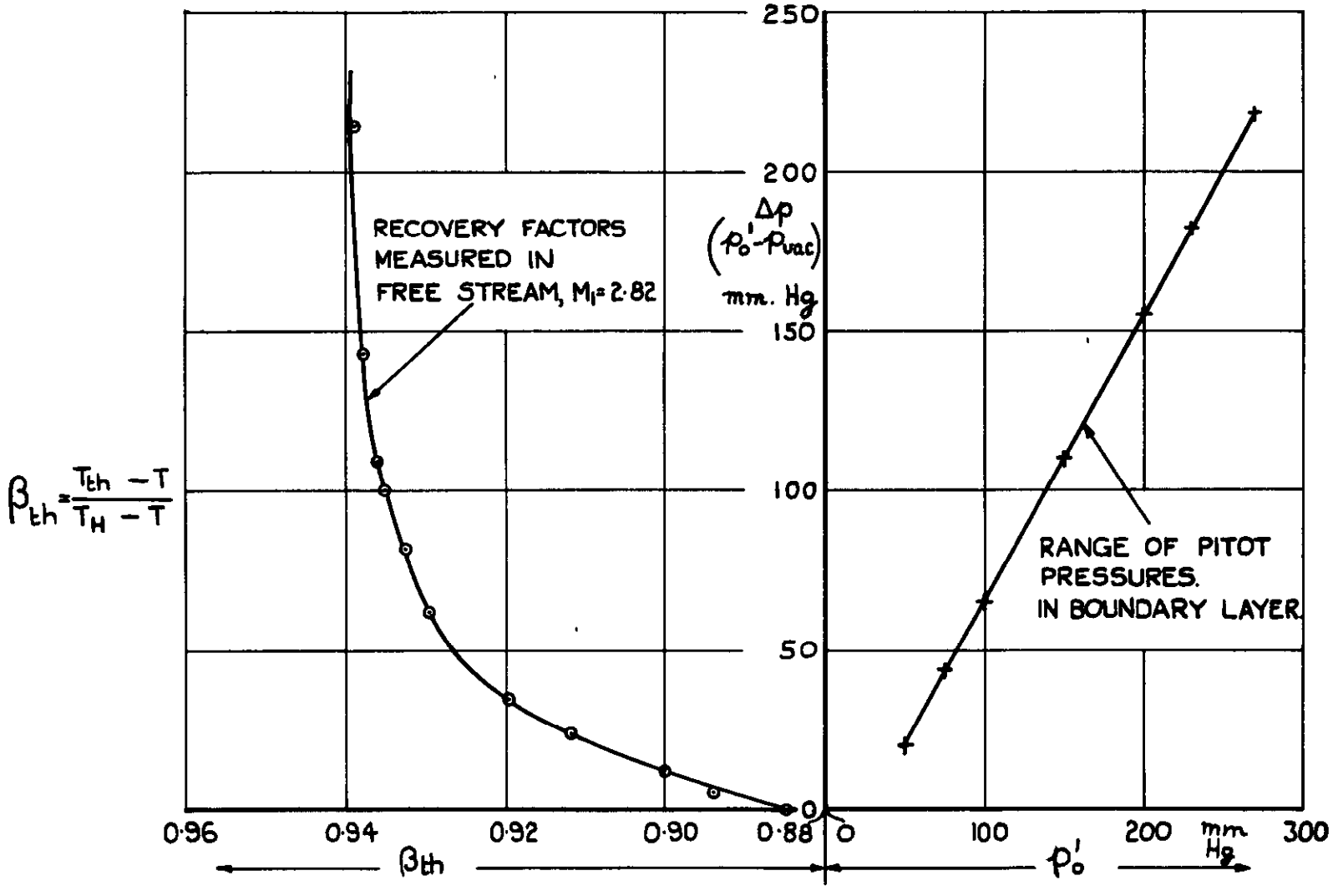

FIG.2. ASSUMED VARIATION OF THERMOCOUPLE RECOVERY FACTOR (β_{th}) ACROSS BOUNDARY LAYER.

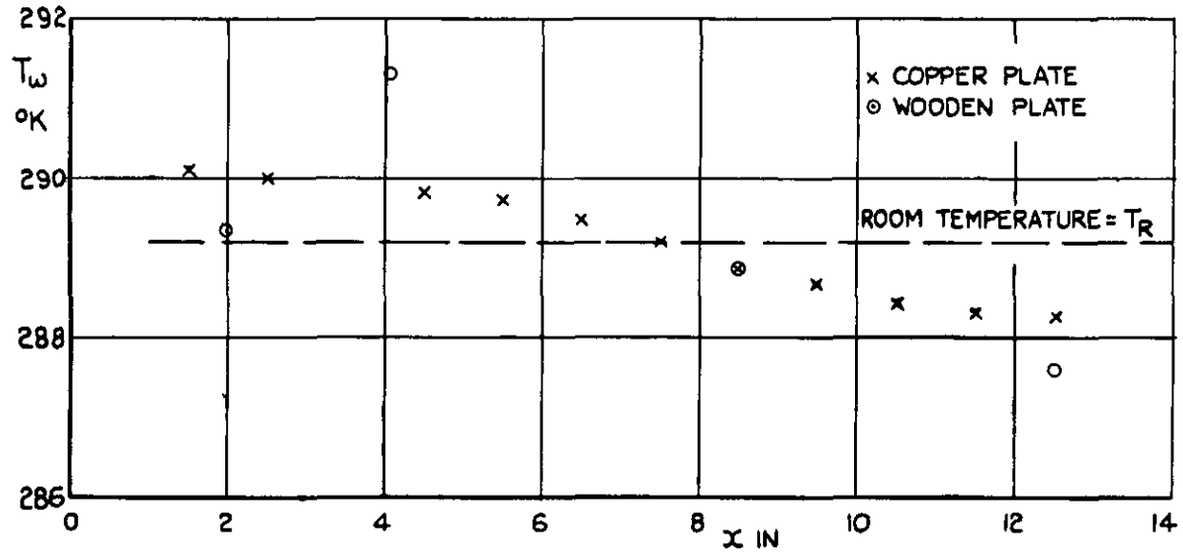

(a) SURFACE TEMPERATURE DISTRIBUTION UNDER ZERO HEAT TRANSFER CONDITIONS. ($T_{HI} = 308°K$)

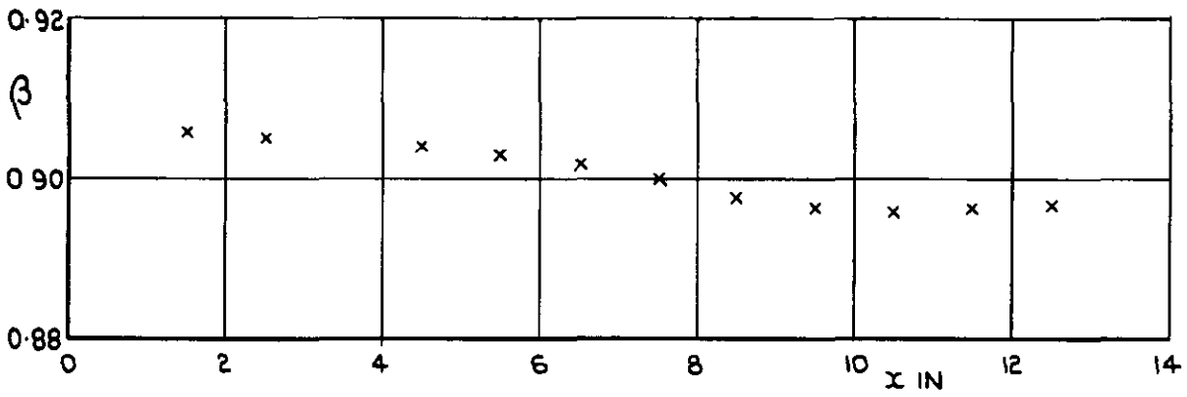

(b) LOCAL RECOVERY FACTORS ON COPPER PLATE FOR MEAN $T_\omega = T_R$ (DERIVED FROM FIG 1 & 3a)

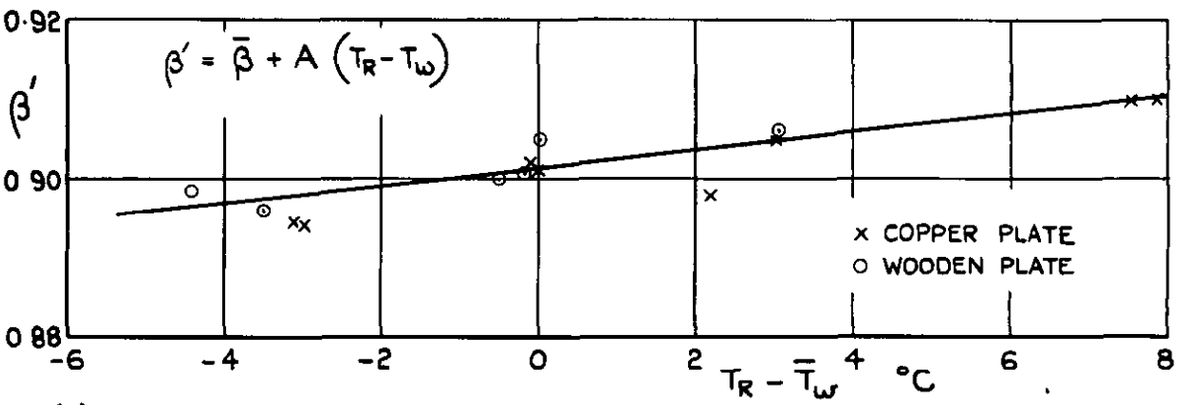

(c) VARIATION OF APPARENT MEAN RECOVERY FACTOR (β') WITH TEST CONDITIONS $M_1 = 2·82$.

FIG.3(a-c) MEASUREMENTS OF KINETIC TEMPERATURE RISE.

FIG.4.

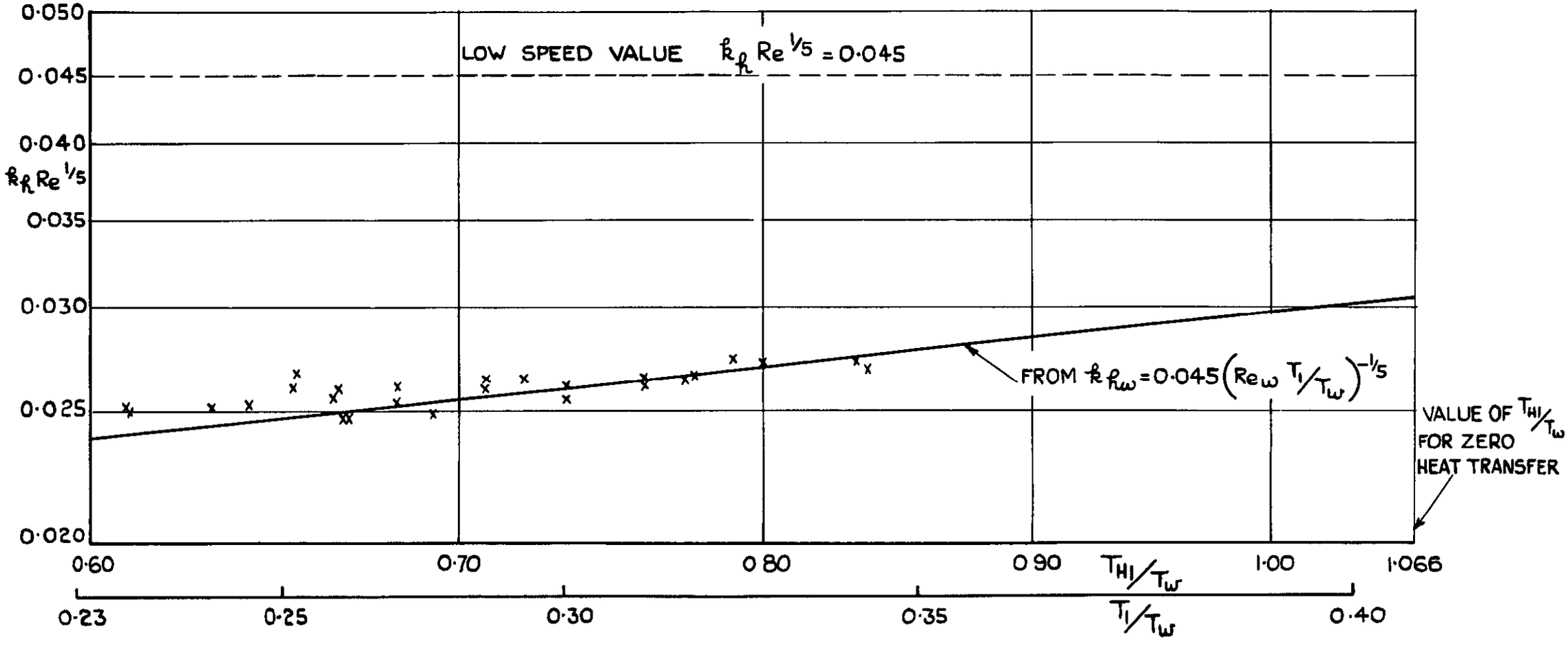

FIG. 4. VARIATION OF HEAT TRANSFER COEFFICIENT WITH TEMPERATURE $M_1 = 2 \cdot 82$.

FIG. 5.

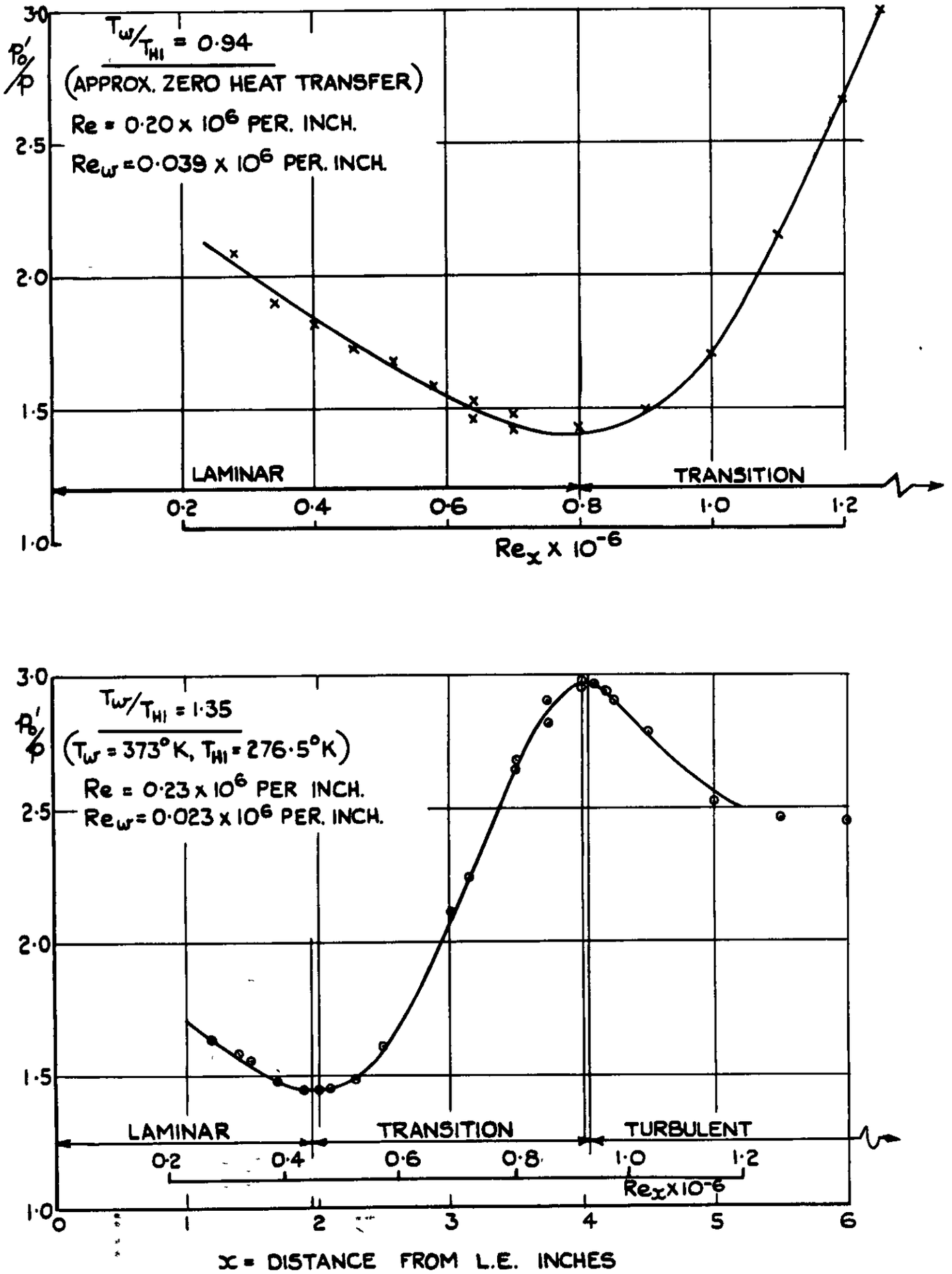

FIG. 5. TRANSITION MEASUREMENTS ON CENTRE LINE OF PLATE.
M_1 = 2·82.

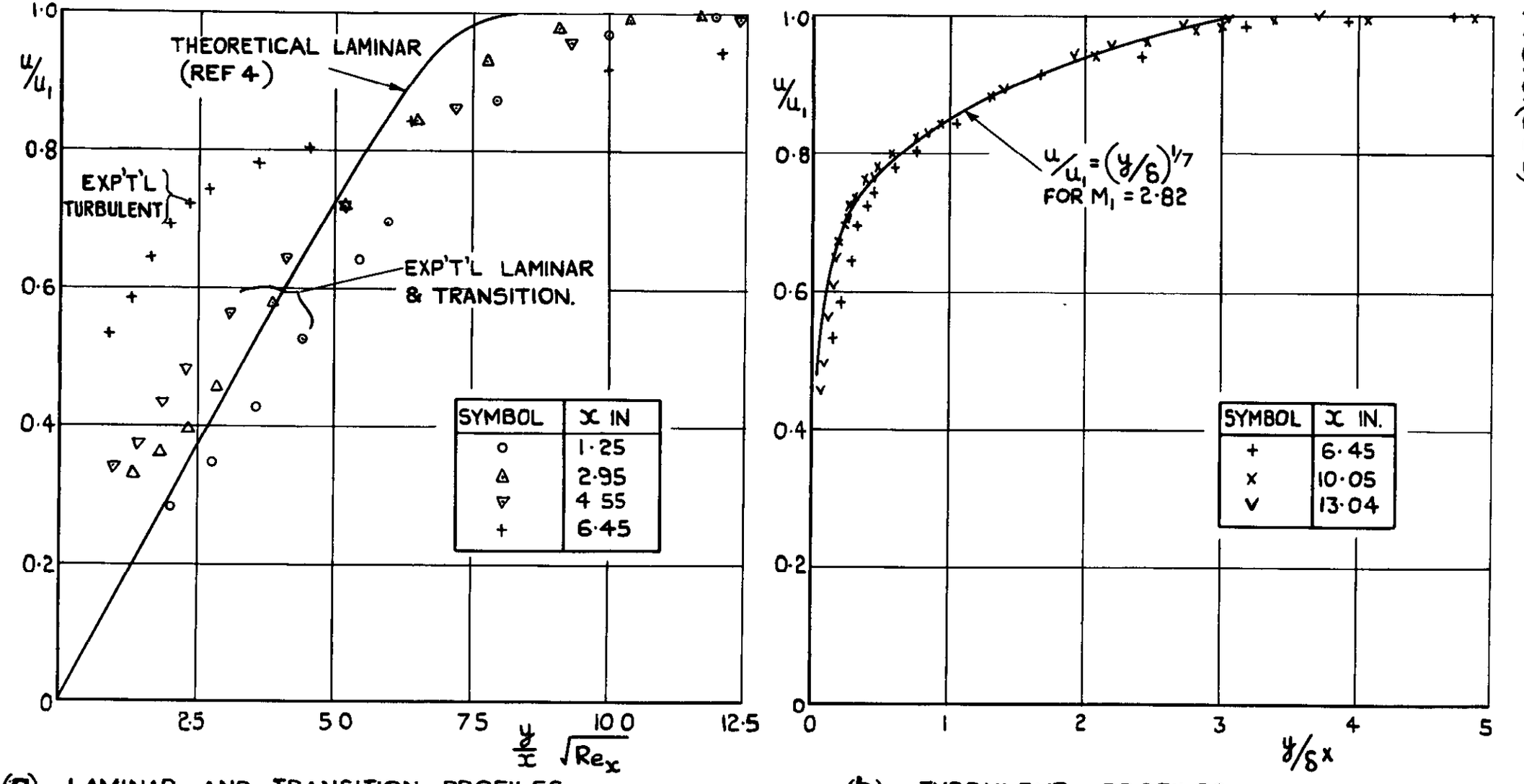

(a) LAMINAR AND TRANSITION PROFILES.

(b) TURBULENT PROFILES

FIG. 6 (a & b) VELOCITY PROFILES ON CENTRE LINE OF PLATE FOR $M_1 = 2{\cdot}82$ AND ZERO HEAT TRANSFER.

FIG.6.(a & b)

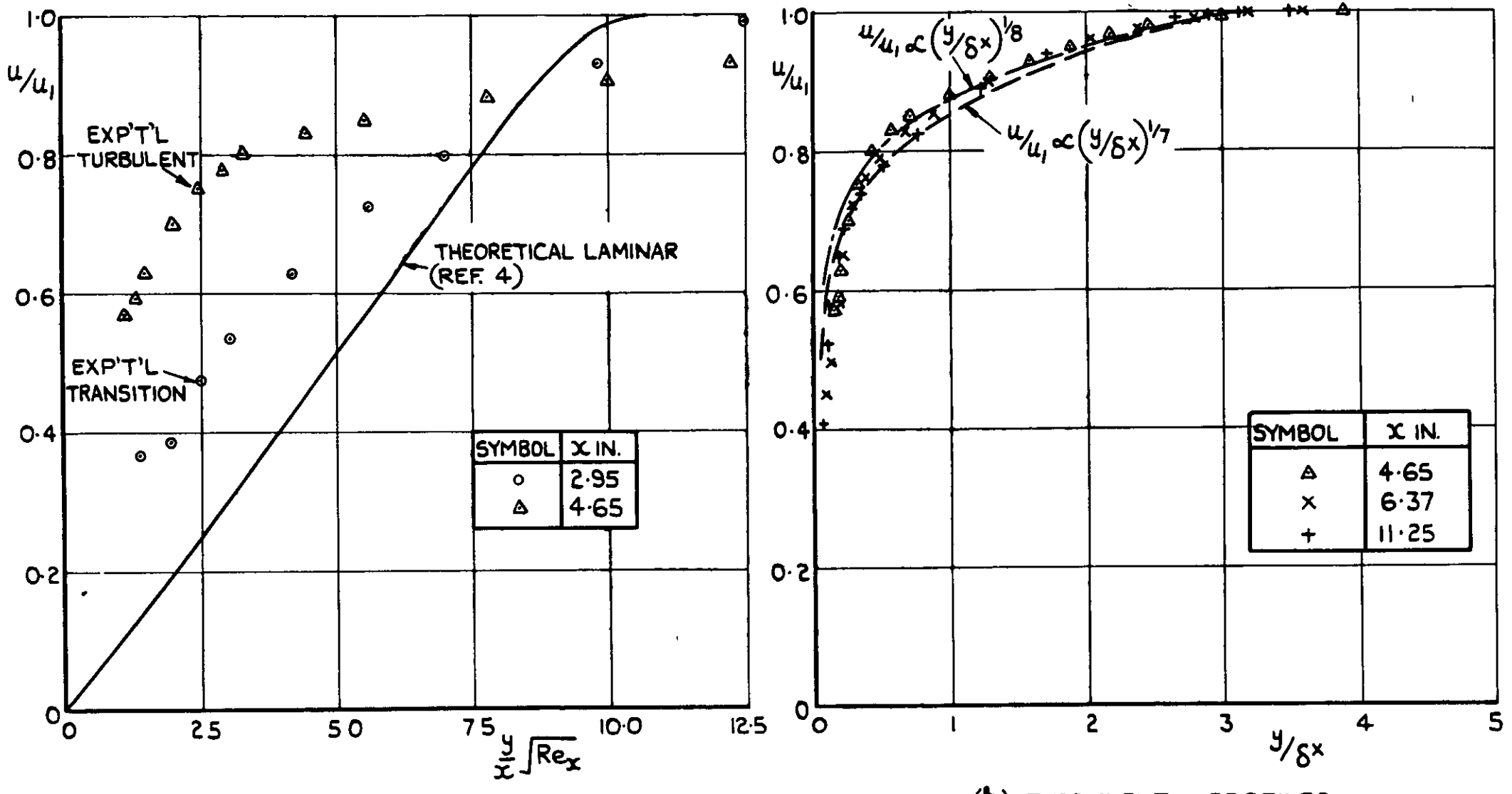

(a) LAMINAR AND TRANSITION PROFILES

(b) TURBULENT PROFILES

FIG.7.(a&b) VELOCITY PROFILES ON CENTRE LINE OF PLATE FOR $M_1 = 2{\cdot}82$ AND $T_w = 373^\circ K$, $T_{H1} = 276{\cdot}5^\circ K$.

FIG.7.(a&b)

FIG.8.

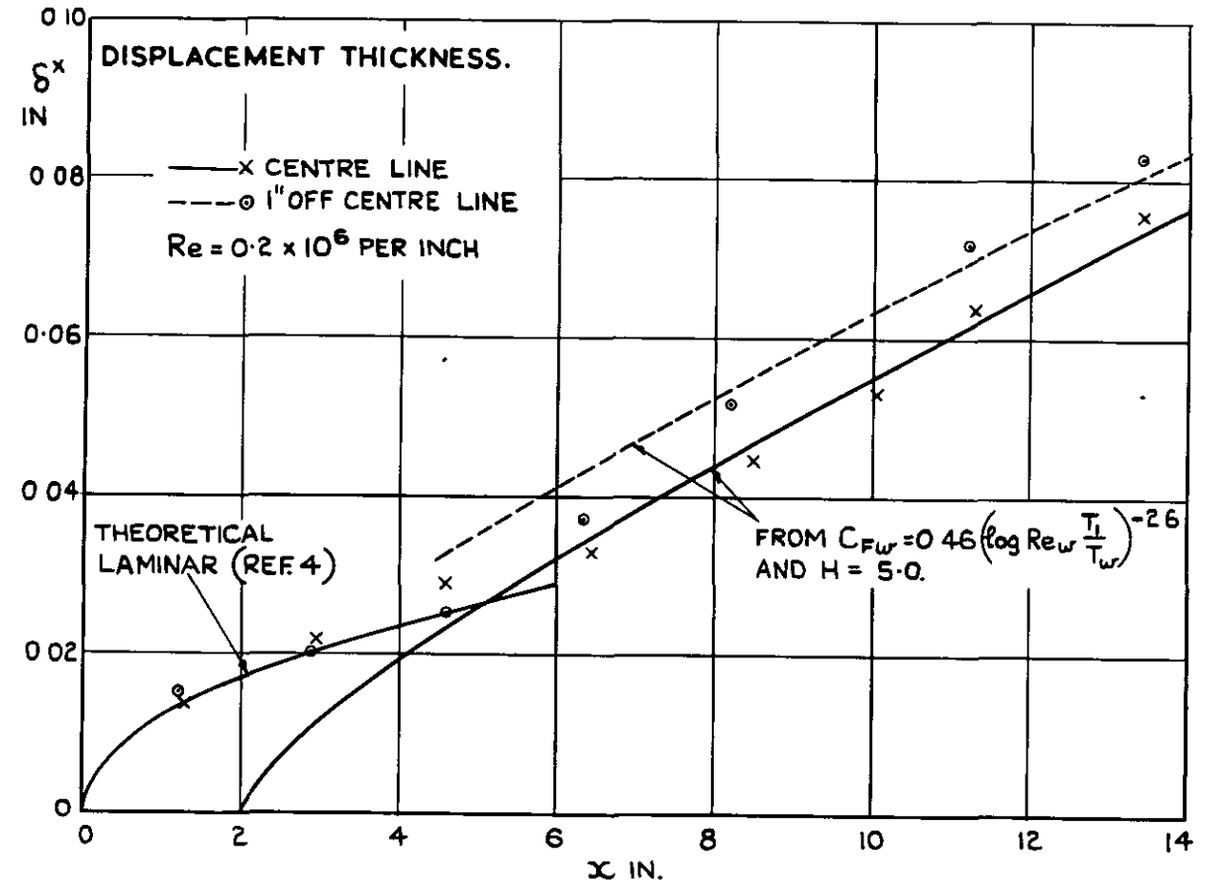

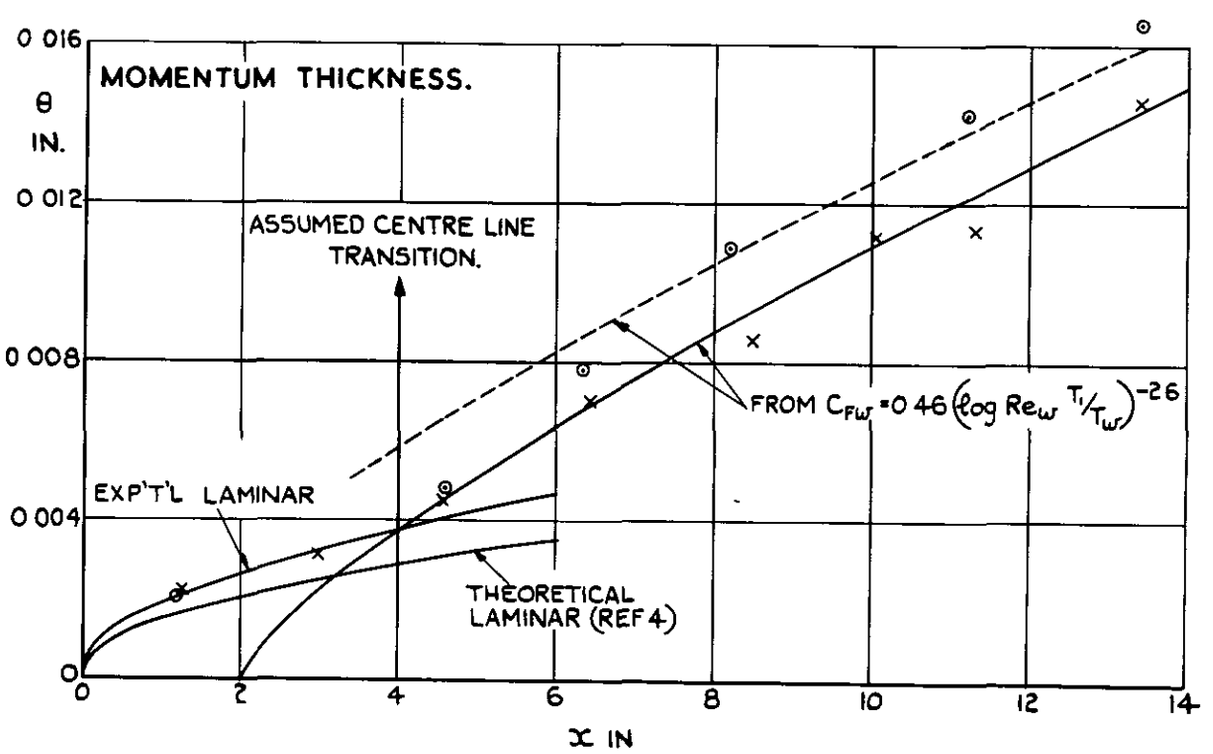

FIG. 8. DISPLACEMENT AND MOMENTUM THICKNESSES.
M = 2·82 AND ZERO HEAT TRANSFER.

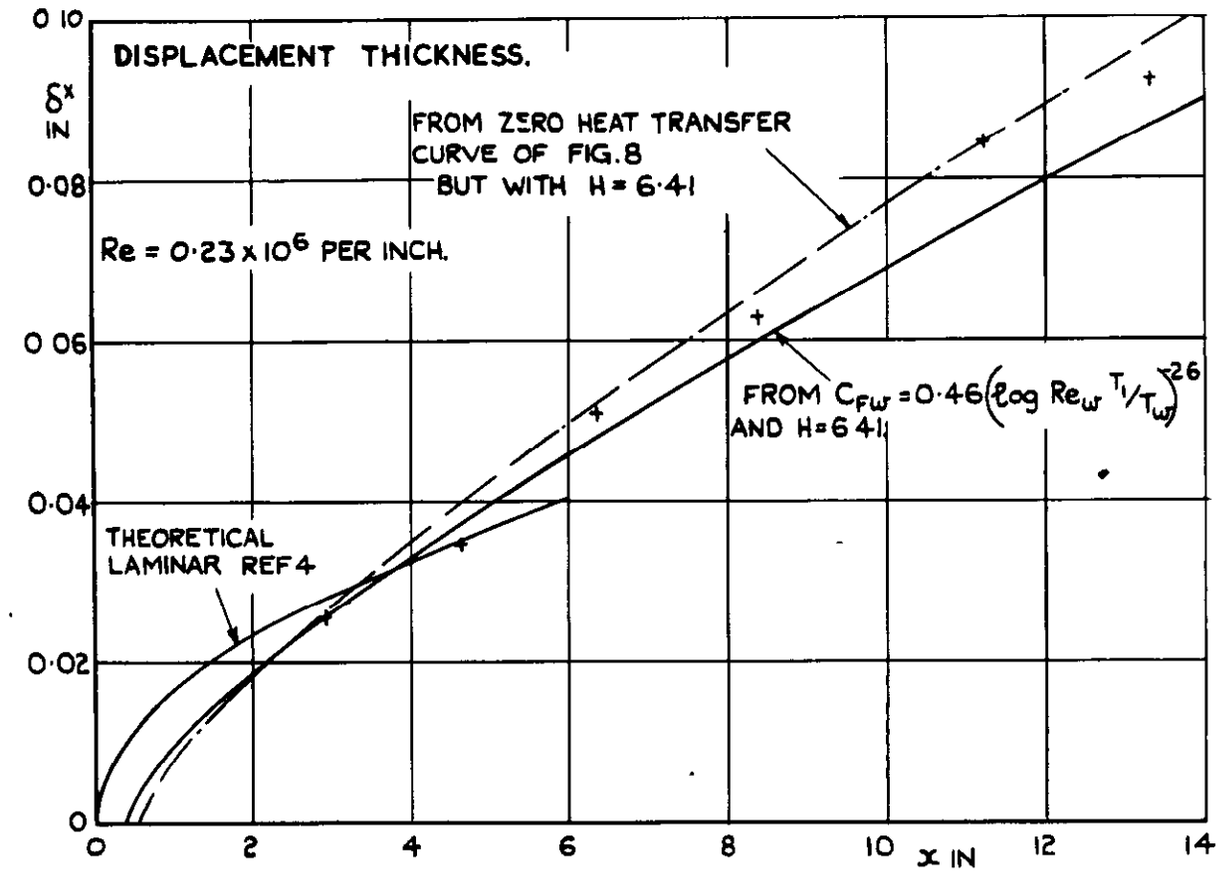

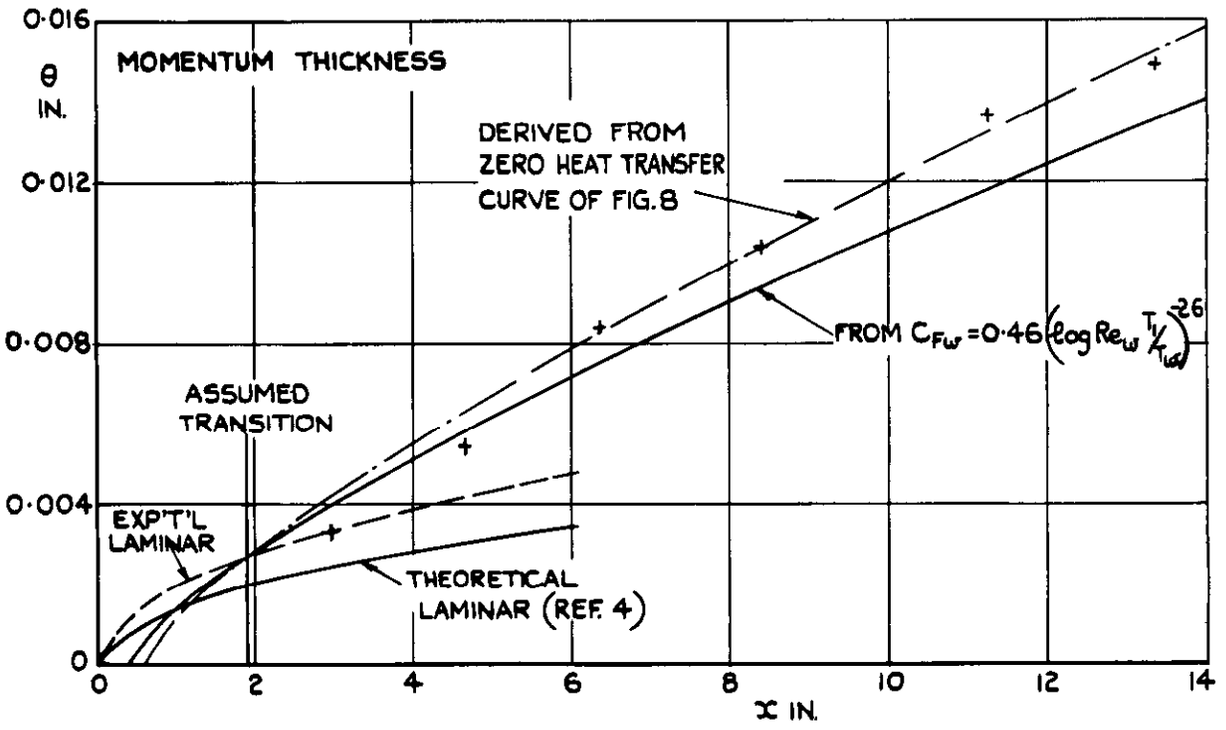

FIG. 9. DISPLACEMENT AND MOMENTUM THICKNESSES
$M_1 = 2·82$. $T_w = 373$ °K. $T_{H_1} = 276·5$ °K.

FIG.10.

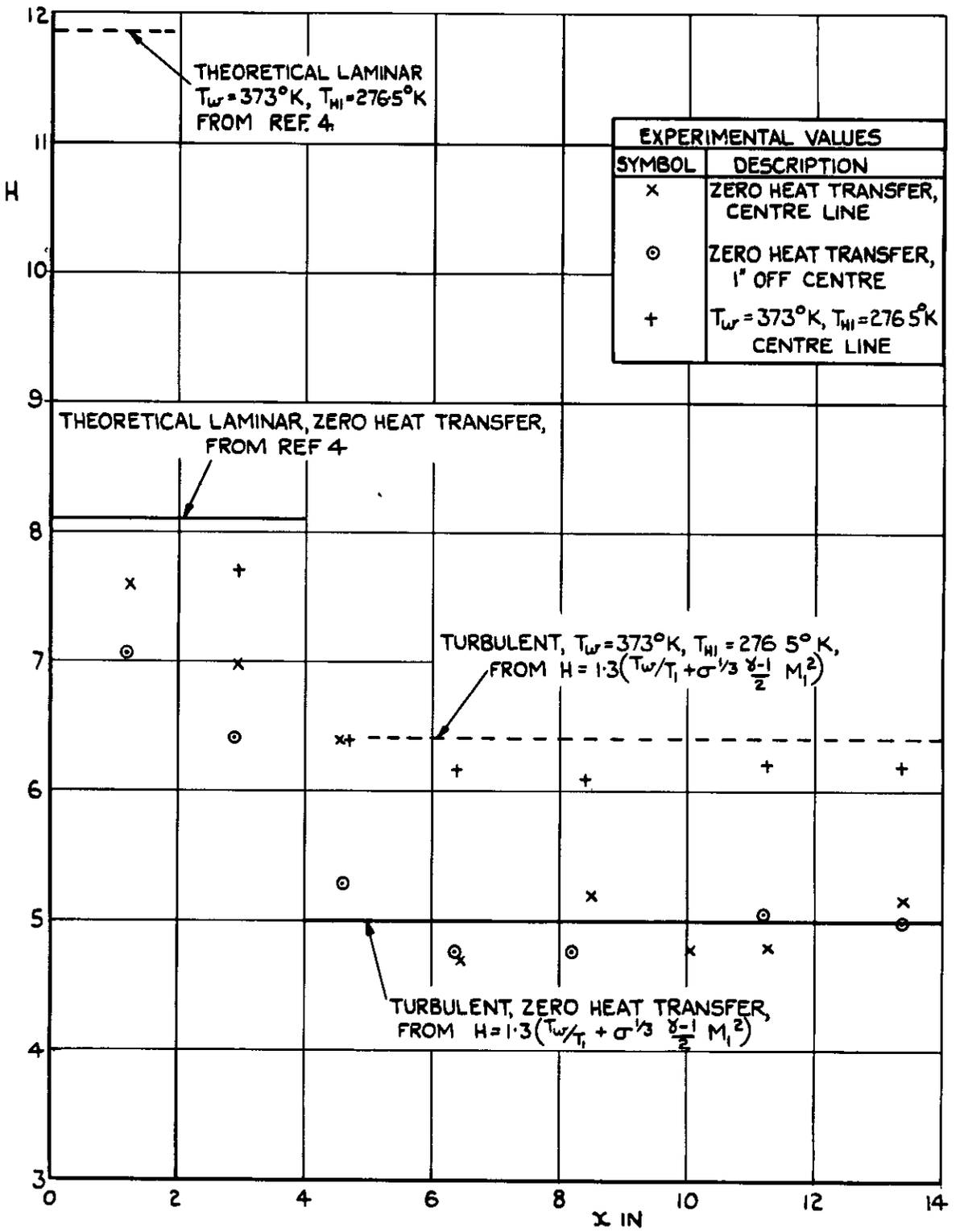

FIG.10. VARIATIONS OF H $(= \delta^x/\theta)$ ALONG PLATE $M_1 = 2{\cdot}82$.

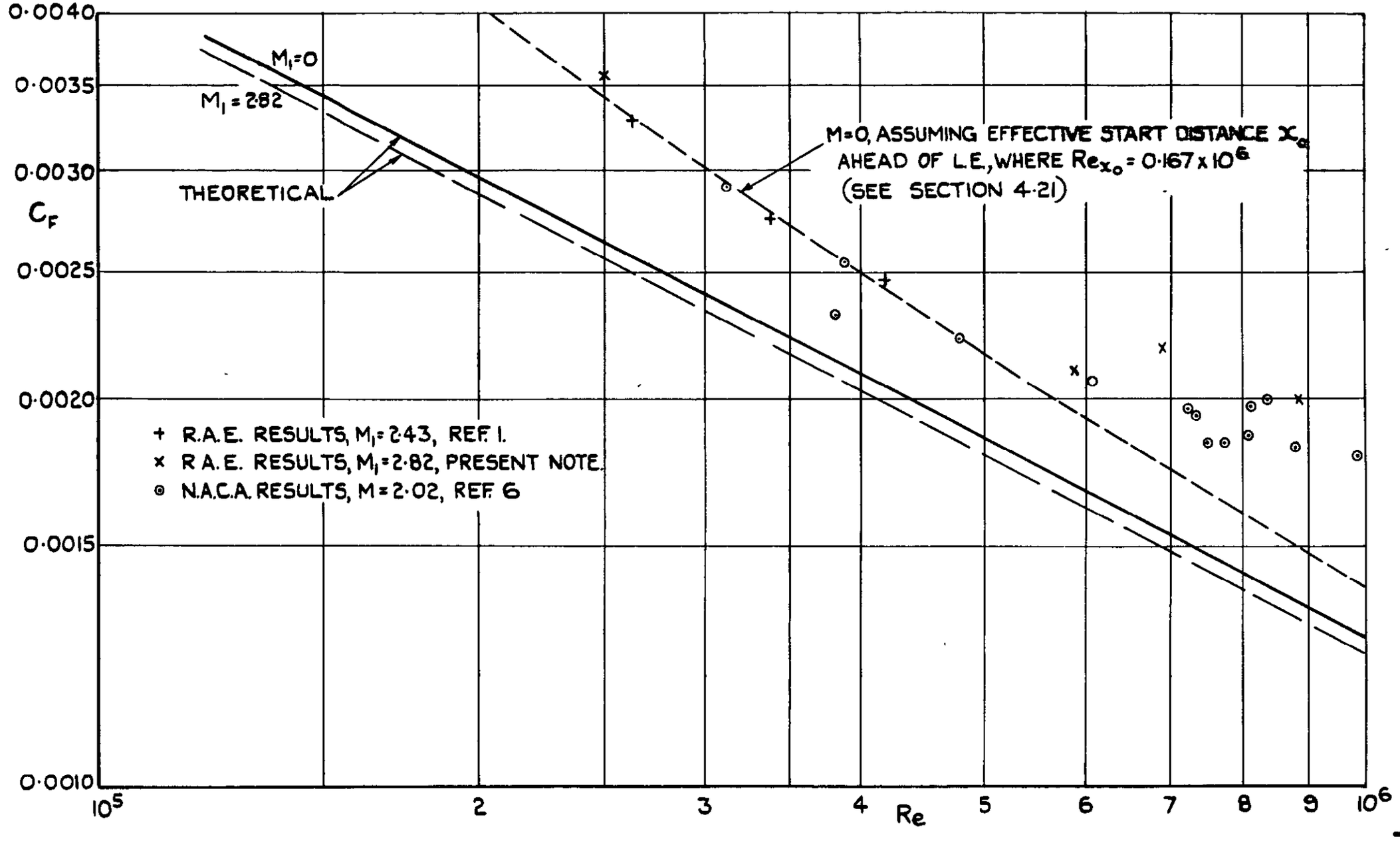

FIG. 11. MEAN SKIN FRICTION FOR LAMINAR BOUNDARY LAYER ON FLAT PLATE.

FIG11

FIG.12.

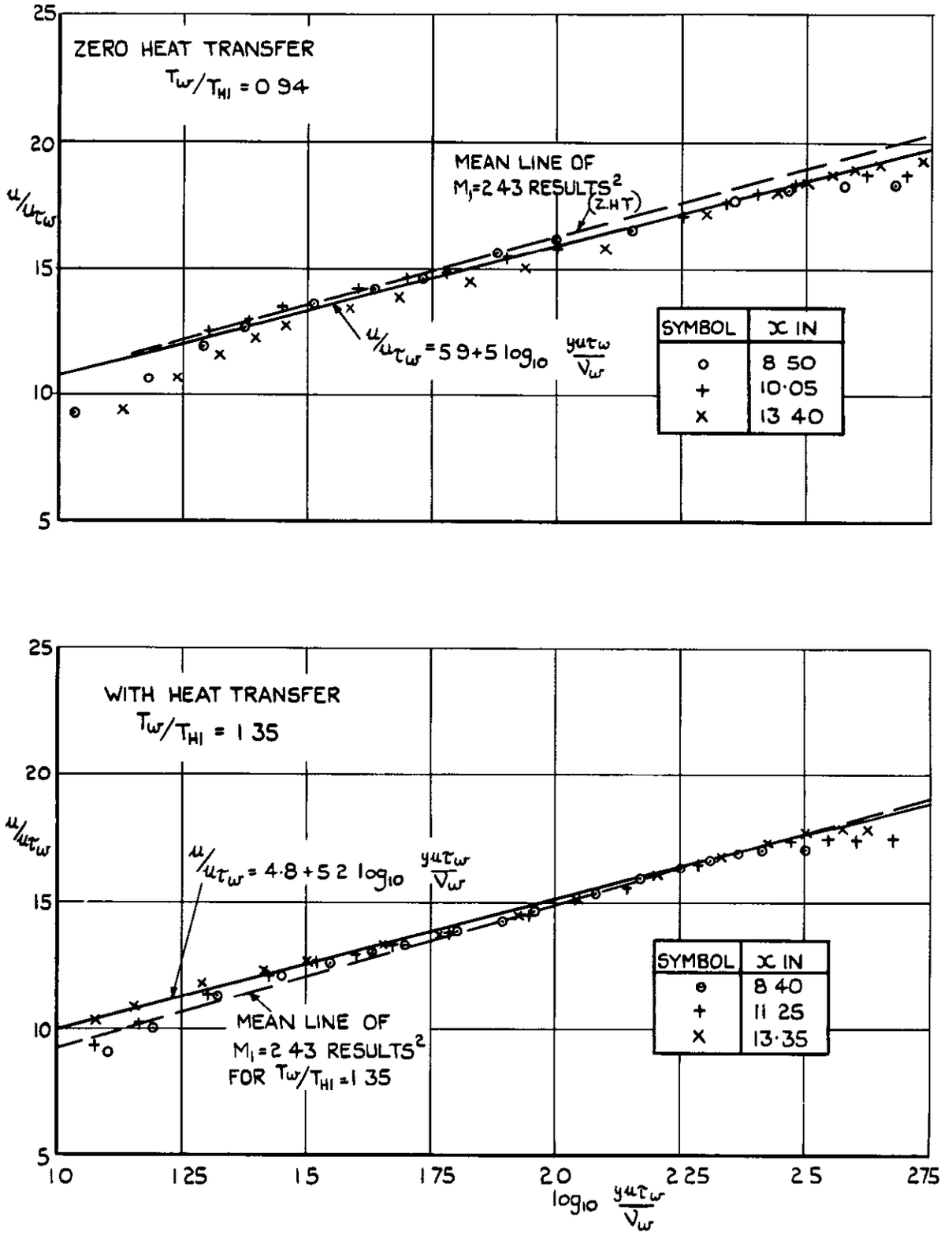

FIG.12. LOG. LAW VELOCITY PROFILES. $M_1 = 2{\cdot}82$.

FIG. 13. (a & b)

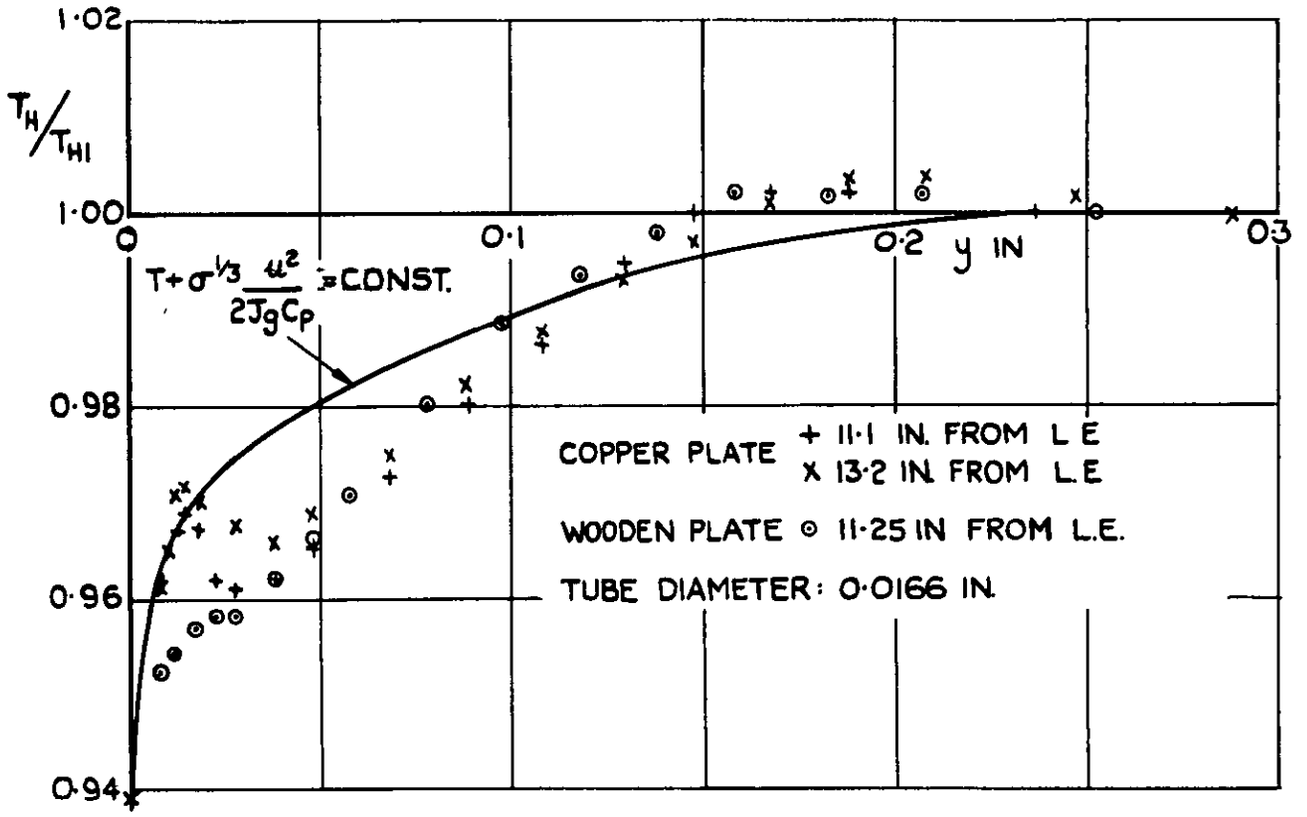

(a) TEMPERATURE DISTRIBUTIONS

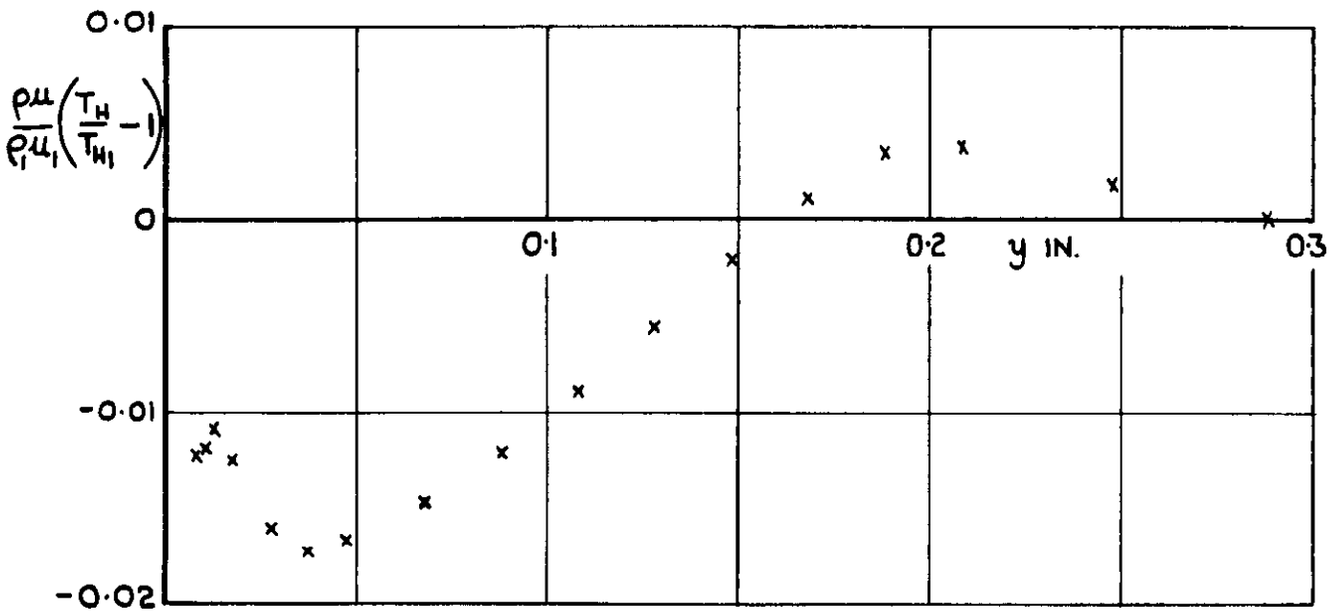

(b) ENERGY DISTRIBUTION, $x = 13·2$ IN.

FIG. 13 (a & b) TEMPERATURE AND ENERGY DISTRIBUTIONS ACROSS ZERO HEAT TRANSFER TURBULENT BOUNDARY LAYER, $M_1 = 2·82$

FIG.14

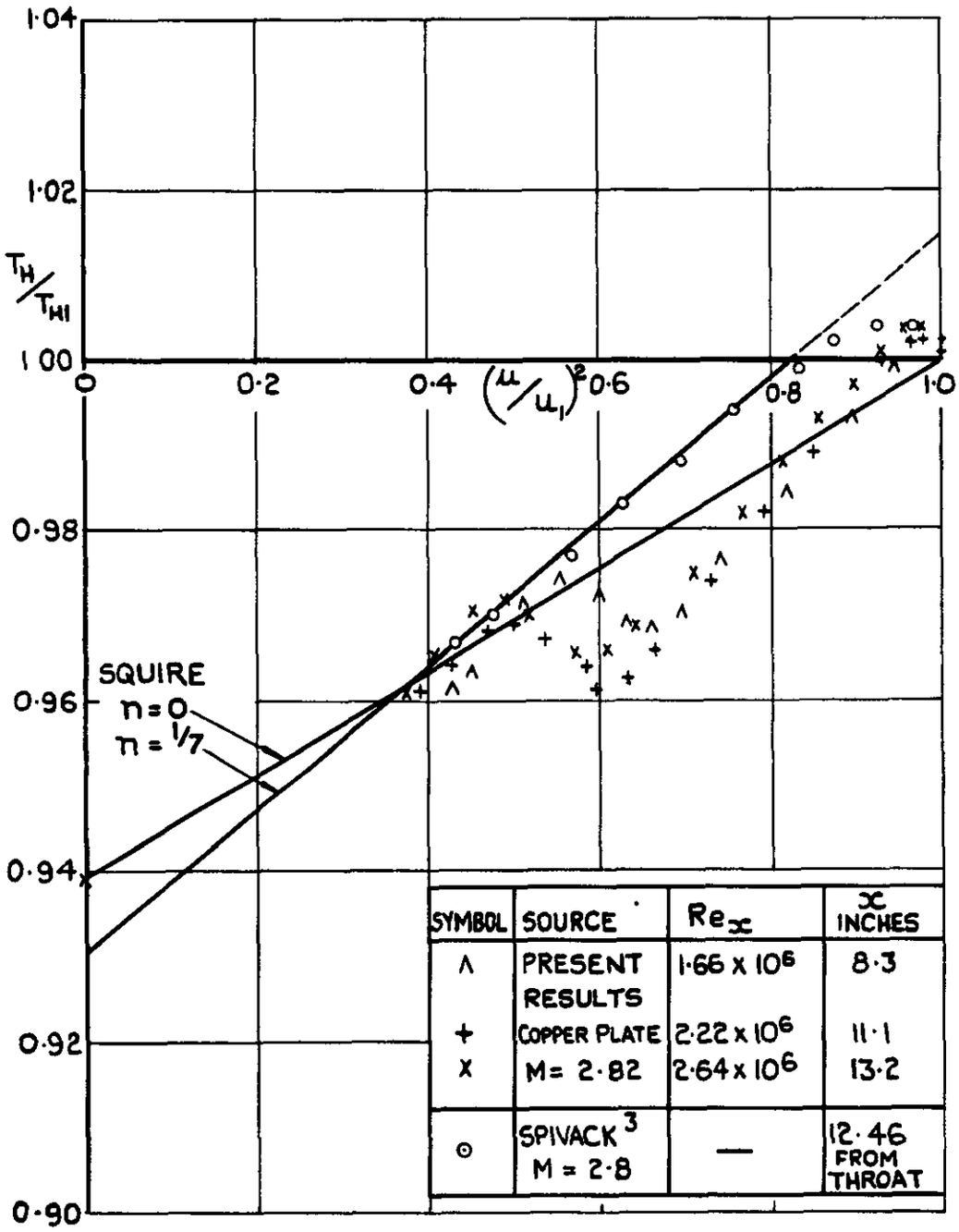

FIG.14 TOTAL TEMPERATURE — VELOCITY DISTRIBUTIONS. ZERO HEAT TRANSFER.

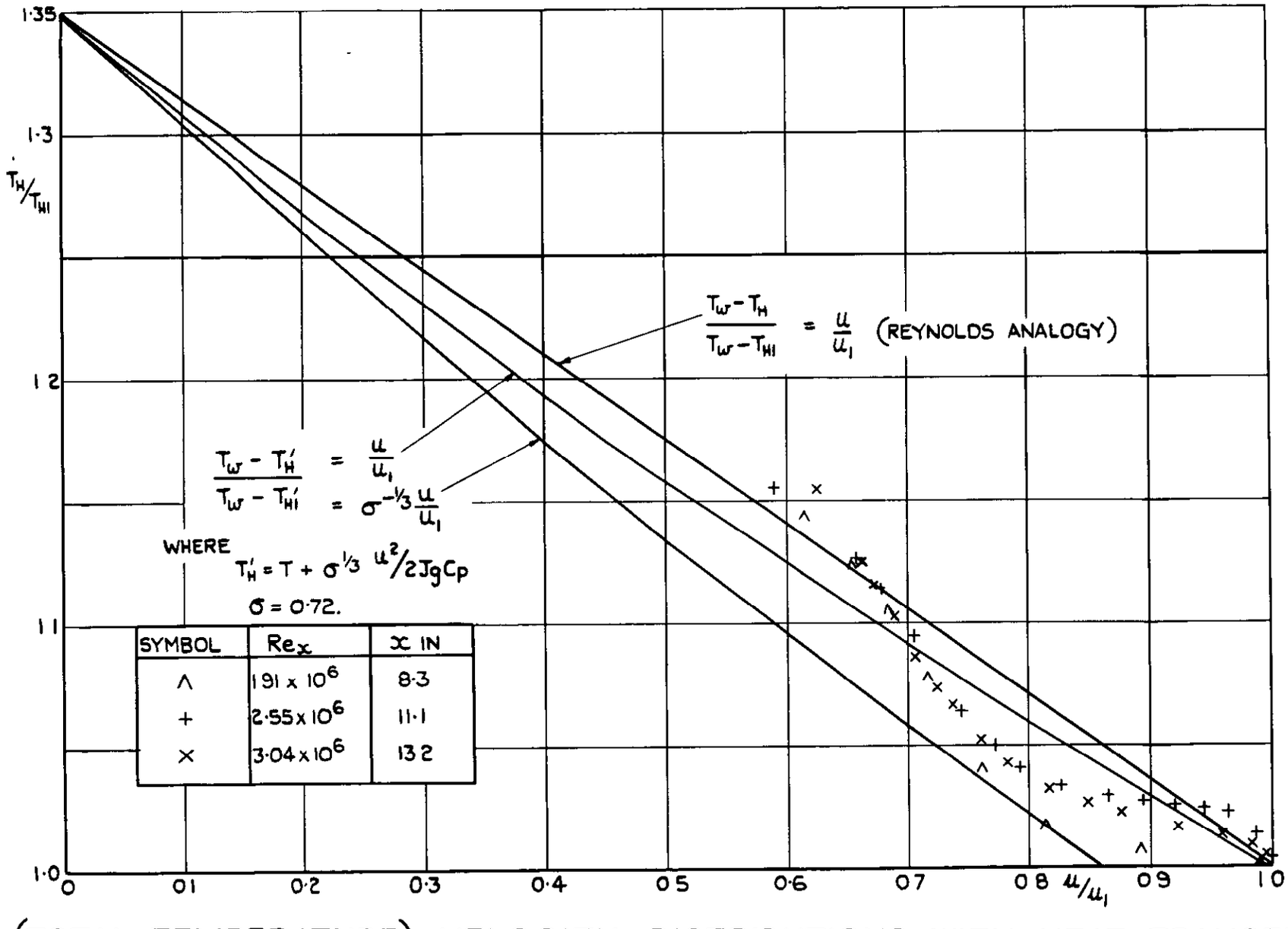

FIG. 15. (TOTAL TEMPERATURE)—VELOCITY DISTRIBUTIONS WITH HEAT TRANSFER.
$T_w = 3·75°K$ $T_{HI} = 276·5°K$.

FIG. 15.

C.P. No. 140
(15,400)
A.R.C. Technical Report

PUBLISHED BY HER MAJESTY'S STATIONERY OFFICE

To be purchased from

York House, Kingsway, LONDON, W C 2; 423 Oxford Street, LONDON, W 1

P O Box 569, LONDON, S E.1

13a Castle Street, EDINBURGH, 2 | 1 St. Andrew's Crescent, CARDIFF

39 King Street, MANCHESTER, 2 | Tower Lane, BRISTOL, 1

2 Edmund Street, BIRMINGHAM, 3 | 80 Chichester Street, BELFAST

or from any Bookseller

1953

Price 8s. 0d. net

PRINTED IN GREAT BRITAIN

S.O. Code No. 23-9007-40